Modeling of room fire growth - Combustible lining materials

Magnusson, Sven Erik; Sundström, Björn

1984

LUND INSTITUTE OF TECHNOLOGY · LUND · SWEDEN
DIVISION OF BUILDING FIRE SAFETY AND TECHNOLOGY
REPORT LUTVDG/(TVBB - 3019)

S E MAGNUSSON - BJÖRN SUNDSTRÖM

MODELING OF ROOM FIRE GROWTH - COMBUSTIBLE LINING MATERIALS

LUND 1984

DEPARTMENT OF FIRE SAFETY ENGINEERING
Institute of Science and Technology
Lund University
Box 118
S-221 00 LUND, Sweden
Telephone +46 46 107360

MODELING OF ROOM FIRE GROWTH - COMBUSTIBLE LINING MATERIALS

Report LUTVDG/(TVBB-3019)

Submitted to the ASTM/SFPE Symposium on Application of Fire Science to Fire Engineering, to be held in Denver, Colorado, in June 1984

Sven Erik Magnusson, Division of Building Fire Safety and Technology, Sweden

Björn Sundström, Swedish National Testing Institute, Borås, Sweden

S. E. Magnusson[1] and B Sundström[2]

MODELING OF ROOM FIRE GROWTH - COMBUSTIBLE LINING MATERIALS

Abstract

A computational procedure has been developed to correlate the room fire test process and results from the proposed ISO small scale laboratory tests. The analysis assumes that the full scale room fire test follows the proposed ASTM method, implying that the lining material covers ceiling and walls. The procedure requires that the heat release measurement response time of the test room is evaluated and for a specific material linked to results from the ignitability test. From the same test, a value of kρc must be calculated. From a small scale rate of heat release test are evaluated specific characteristics describing the RHR-curve. The derived test room and material characteristics are used as input data to an uncomplicated mathematical expression, essentially describing the full scale test fire process as a concurrent flame spread phenomenon. Undetermined parameters in the model have been derived

---

[1]Division of Building Fire Safety and Technology, Lund Institute of Technology, Sweden

[2]Swedish National Testing Institute, Borås, Sweden

using regression analysis and results from seven full scale room tests. In these the tested materials were of such thickness that no burning through occurred. The quantitative accuracy was thought acceptable but further experimental confirmation and sensitivity studies are needed to assess the inherent variability. Qualitatively the procedure predicted the same relative ranking of materials as the room test.

For thin surface finish materials on a non-combustible base it was possible to derive a radically simple expression to be used as indication of the risk of flashover. Again, the final usefulness can only be evaluated on the basis of further experimental evidence.

In summary, it is thought that a first step has been taken in the efforts to use results from small scale tests to rationally predict full scale fire growth (for one specified scenario) and rank materials.

Key words: Combustible lining material, small scale test, full scale test, correlation study, mathematical models, design models.

Nomenclature

A area

a $h^2/k\rho c$

B mass transfer number

c specific heat

h heat transfer coefficient (total)

k	thermal conductivity
L	heat of vaporization
$\dot{m}''$	mass loss rate
$\dot{Q}''$	rate of heat release per unit area[1)]
$\dot{q}''$	rate of heat transfer per unit area
r	mass consumption number (Ref. /22/)
r_{ox}	mass oxygen/fuel stoichiometric ratio
T	temperature
Y_{O_2}	mass fraction of O_2
α	undetermined parameter in Eq. 23
α'	$\ln\alpha$
β	undetermined parameter in Eq. 23
ε	absorptivity of surface
θ	temperature rise
λ	rate of heat release curve decay coefficient
ρ	density
χ	degree of complete combustion
ΔH	heat of combustion

Subscript

a	ambient
b	burning
c	convective
e	externally impressed
f	flame
rt	room test
s	surface

---

1) $\dot{Q}''$ (without subscript) refers to rate of heat release from small scale test

The compartment fire growth and fire spread has been a subject of extensive investigations, experimental and theoretical, during the last decade. For the case when the burning item is an isolated or single object such as a bed, an upholstered chair, etc, research has on the whole been successful and given a quantitative understanding of the physical phenomena involved. Within the area of fire growth and combustible linings progress has been much slower, despite the fact that this has been a problem of concern to the legislators and authorities since the advent of building fire safety regulations. As a consequence, there still exists no internationally accepted basis for a functional classification of surface finishes.

The work in this area can be divided into three interacting lines of development. The first concerns the generation of improved small scale test methods. From an international, and perhaps especially European, point of view the work carried out within the International Standardization Organization (ISO) is of importance as it opens the way for the replacement of the multitude of national test standards with internationally agreed ones. The second one relates to the development of a full scale room test procedure, initiated within ASTM and taken up by ISO. The third trend concerns the evolution of mathematical modelling, both of the fire process in the small scale laboratory apparatuses and the full scale fire growth.

These three lines give the structure of the Swedish research

project which is the subject of this report.

Regarding the extensive work carried out within ISO in order to generate tests for measuring "reaction to fire" of building materials, references /36/ and /37/ give a general review of the historical background, the philosophy of hazard assessment by testing methods and the possible use of specific tests to derive material flammability characteristics for use in fire environment modelling.

OBJECTIVE AND EXTENT OF THE PROJECT

The objectives of the project were three-fold: utilize the proposed ISO tests to derive basic flammability characteristics which could rationally be used as classification criteria, to generate a full scale fire test standard and, finally, to mathematically correlate small scale test data and the full scale fire process. For this purpose, thirteen materials were tested in eight small scale tests, in the full scale test room and in a one-third scale version of this room. Table 1 lists the materials and Table 2 the test methods. The project is part of a larger one, described in /1/, carried out jointly by the Swedish National Testing Institute and Lund Institute of Technology.

When the report is being written (February 1984) the analysis of the experiments has not been finalized. This is therefore a progress report where results are preliminary and incomplete and subject to a continuing evaluation.

BASIC FLAMMABILITY PARAMETERS

Various lists of these parameters have been published. An example is the analysis in /10/, which concludes with the following enumeration

(1) thermal inertia $\sqrt{k\rho c}$

(2) "creeping" flame spread coefficient C

(3) minimum radiant flux for ignition $\dot{q}''_{o,ig}$

(4) minimum radiant flux for flame spread $\dot{q}''_{o,\infty}$

(5) heat of reaction ΔH

(6) stoichiometric oxygen to fuel ratio $r_{o\infty}$

(7) heat of vaporization L.

In this report, and because of the chosen full scale room test scenario, we will concentrate our discussion to the results obtained from the ignitability and rate of heat release apparatuses (methods 1,4,5 in Table 2). The proposed ASTM room test method, upon which the full scale experiments were designed, assumes that the lining material covers walls and ceilings. Obviously, in real life situations a common practice is to put lining only on the walls. For this case, the modelling will have to be based on parameters derived from the "creeping" surface spread of flame test methods analysed in /11/ (parameters C, $\dot{q}''_{o,ig}$ and $\dot{q}''_{o,\infty}$ in the list above).

This report will concentrate on the relation between small scale tests and the full scale room fire growth. Future

reports from the project will give a detailed account of the full analysis.

IGNITABILITY TESTS

Test procedure apparatus

The test - ISO TC92 TR5657, Fire Tests, Reaction to Fire, Ignitability of Building Products - is outlined in Fig. 1.

The test is performed by exposing horizontal specimens to constant irradiance $\dot{q}''_e$ at specified levels ranging from 10 kW/m² to 50 kW/m². The irradiance is provided by an electrically heated radiator cone positioned above the specimen. The cone has a hole at the top to avoid trapping any combustible gases. A pilot flame is applied once every 4 s to a position 10 mm above the surface of the specimen to ignite any volatile gases.

A specimen and a counterweight system ensure that the specimen is kept in position and receives constant heat flux during the test.

The sample is placed on a silicate base board and the test specimen is formed by wrapping aluminium foil around the sample (except for the exposed surface) and the base board.

Five replicate tests were performed on each irradiance level, 10, 20, 30, 40 and 50 kW/m².

Thermocouples were attached to the sample surface, between the sample and the baseboard, at the rear side of the baseboard and on top of the specimen pressing plate as shown in Fig. 2.

Modelling of the test process

The main quantitative information obtainable from the ISO Ignitability Test is a set of values of t_{ig} - ignition time - for a set of exposure radiation levels $\dot{q}''_e$ in the range $\dot{q}''_e$ = 0-5 W/cm² - usually but not necessarily with an igniting flame present.

Data from the ignitability test can be used for different purposes. The immediately available ignition time values can be regarded as hazard indices in themselves. Methods of deriving the indices are suggested in /2/ and /12/. Data can also be extrapolated to yield useful quantities such as minimum level of impressed flux to cause ignition. Finally, and with the supplementary temperature measurements described earlier, test output can be used to derive important material and process parameters such as thermal conductivity k and thermal capacity ρc of the tested specimen. A prerequisite is a model of the test process.

Ignition is generally a gas phase phenomenon; the gases being produced by the heating of the solid which leads to decomposition (pyrolysis) and the diffusion of gaseous volatile products through the material and across its surface. If produced at a sufficient rate in an atmosphere which support exothermic reactions they may ignite sometimes without, sometimes with,

the presence of some (pilot) additional energy. The chemical mixing processes usually determine whether ignition can occur - but, if it can, it is usually the thermal and other physical properties (such as melting point) of the solid that determine the time. This because the rates of chemical processes vary with temperature so much that for many practical purposes one can regard them as being effectively negligible below a certain narrow range of temperature and producing gaseous fuel in abundance above that narrow range.

Thus, one can, for many practical purposes, treat ignition as occurring above particular surface temperature. This temperature is a practical quantity, varying with material, and with the absence or presence (and position) of an igniting pilot source.

Complementary to the thermal ignition model is the theory put forward in e.g. /13/ that ignition requires that the flow rate of pyrolyzed volatiles must exceed a specified minimum level.

Going back to the thermal ignition model and the heat conduction problem, the materials can often be considered as semi-infinite; i.e. they have a thickness large enough for their behaviour to be unchanged by added thickness. For this to be valid, the specimen thickness d should be

$$d >> k(T_{ig} - T_a)/\dot{q}''_e \qquad (1)$$

where

T_{ig} = the effective ignition temperature

T_a = the initial or ambient temperature

$\dot{q}''_e$ = the level of impressed flux

i.e. the applicability of the concept of thermal thickness is dependent on exposure level.

For a thermally thick specimen, the degree of accuracy of the computed solution varies with the assumptions that are being made regarding thermal properties and boundary conditions. The ordinary custom is to treat thermal properties as constant in time and temperature and neglect changes in surface absorption, and the results presented here will be based on these assumptions. Regarding boundary conditions these may be described by a three separate approximations, leading to solutions of varying degree of realism and computational complexity. It is instructive to study how theory and practice compare for the separate choices of boundary conditions.

The one-dimensional heat conduction equation is written

$$\rho c \frac{\delta \theta}{\delta t} = \frac{\delta}{\delta x}\left[k \frac{\delta \theta}{\delta x}\right] \qquad (2)$$

where $\theta = T - T_a = 0$ for $t=0$ and the generalized heat flux boundary condition is written

$$-k \frac{\delta \theta}{\delta x} = \varepsilon[\dot{q}''_e - h_\varepsilon \theta_s - \sigma((\theta_s + T_a)^4 - T_a^4)] = \dot{q}''_s(\theta_s, \dot{q}''_e, t) \text{ for } x = 0 \qquad (3)$$

where

ε = absorptivity of the surface

$h_\varepsilon = h_\infty/\varepsilon$ = convective heat transfer (cooling) coefficient h_∞ divided by ε

θ_s = surface temperature rise

σ = Stefan-Bolzmann constant

$\dot{q}''_e$ = the prescribed impressed heat flux

$\dot{q}''_s$ = the effective heat flux into the solid

T_a = ambient air temperature.

Exact analytical solution of Eqs. 2 and 3 is not possible. It is therefore usually assumed that either surface cooling can be totally neglected (i.e. $\dot{q}''_s = \dot{q}''_e$) or that the non-linear boundary equation can be linearized by writing (for $x = 0$)

$$-k \frac{\delta\theta}{\delta x} = \varepsilon(\dot{q}''_e - h\theta_s) \qquad (4)$$

where

$$h = \sigma \frac{(\theta_\sigma + T_a)^4 - T_a^4}{\theta_s} + h_\varepsilon \qquad (5)$$

is assigned a constant, average value.

In the first case, increase in surface temperature θ_s is given by the simple expression

$$\theta_s = \frac{2}{\sqrt{\pi}} \dot{q}''_e \sqrt{\frac{t}{k\rho c}} \qquad (6)$$

In the second case surface temperature rise is given by

$$\theta_s = (\dot{q}''_e / h)\, F(t) \qquad (7)$$

with

$$F(t) = 1 - \exp(at)\,\mathrm{erfc}\sqrt{at} \qquad (8)$$

where the parameter a

$$a = h^2/k\rho c \qquad (9)$$

When using Eq. 5 it is essential that the constant value h of the total heat transfer coefficient is chosen with regard to the surface temperature interval being considered. Guidelines are given e.g. in /11/.

The dimensionless quantity (at) is linked to the governing heat conductivity Fo- and Bi-numbers by the expression $at = Fo\,Bi^2$ and is a non-dimensionalized time parameter of fundamental importance for the problem being considered.

Equations 6 and 7 have been extensively used in the fire literature. For the non-linear case (Eq. 3) no closed solutions are possible. Approximate methods must be employed. If a purely numerical solution is not justified (either because of the programming effort or because that kind of approach inherently provides little insight into the physical significance of involved parameters) approximate analytic methods are useful. One of these is the so-called integral method. The basic steps in the method are explained in most textbooks on the subject see e.g. /14/, where also an example gives the solution of Eqs. 2 and 3. It is demonstrated that the relation between

surface temperature rise θ_s and time t is given by the numerical evaluation of an integral. In /15/, it is shown that one of the expressions under the integral sign varies slowly and can be replaced by a constant. The final relation between θ_s and t is then given by /15/

$$t = U\left[\frac{\theta_s^2}{\dot{q}''} + \frac{\tau}{\gamma^{3/2}} \ln\frac{(2s\theta_s + \tau - \sqrt{\gamma})(\tau + \sqrt{\gamma})}{(2s\theta_s + \tau + \sqrt{\gamma})(\tau - \sqrt{\gamma})} - \frac{\theta_s(\tau + 2s\theta_s)}{\gamma \dot{q}''_\varepsilon}\right] \quad (10)$$

where

$$U = \frac{2}{3}\frac{k\rho c}{\varepsilon^2} \quad (11a)$$

$$\tau = -(h_c/\varepsilon + 4\sigma T_a^3) \quad (11b)$$

$$s = -\frac{25}{3}\sigma T_a^2 \quad (11c)$$

$$\gamma = (\tau^2 - 4\dot{q}''_e s) \quad (11d)$$

and

$$\dot{q}''_\varepsilon = \dot{q}''_e/\varepsilon = \dot{q}''_e + \tau\theta_s + s\theta_s^2 \quad (11e)$$

Eq. 10 demonstrates the invariate or scaling properties of the factor $t/k\rho c$. The equations 10-11 will constitute the basis for experimental determination of $k\rho c$.

Extraction of material property data

Fig. 3 gives an example of how the various mathematical modelling approaches compare with process measurements when mate-

rial property data and boundary conditions are assumed to be known. The experimental curves were obtained during a series of tests to find the best thermocouple application for measuring surface temperatures. The tested materials were boards of Monolux, a standard silicate material with assumably known thermal properties. Curve 1 gives the surface temperature rise according to Eq. 6, curve 2 according to Eq. 10, curve 3 is a numerical, finite difference solution, curve 4 is the experimental result and curve 5 gives the solution of Eq. 7 with h = 30 W/m^2 K. The solution procedure used to calculate curve 3 will be shortly described later on. Regarding curve 5 with h arbitrarily chosen = 30 W/m^2 K a value of h = 20 W/m^2 K would have given a substantially better agreement with the experimental results. It should also be remarked that the surface thermocouple arrangement shown in Fig. 2 may indicate temperature values which are somewhat low during especially the initial stages of the experiment.

Curves 6 and 7 refer to temperature 13 mm inside the material.

Fig. 3 outlines surface temperature curves of varying accuracy that can be computed when thermal properties are known. In reverse, minimizing the difference between modelling and experimental output is a well-established procedure for obtaining process and material property data. A number of methods are available for this extraction of information. The dynamics of the heat diffusion can be determined using system identificaton methods /16/. Another approach utilizes measured temperatures transformed via the Laplace integral. Solution of the heat conduction equation by the Laplace method gives the cor-

responding theoretical values and a basis for comparison /17/. A third mode of procedure, and the most common one, is to directly match modelling and experimental output. The problem of determining material thermal properties has ben studied for at least a hundred years and developed into standard laboratory techniques, in most cases based on this methodology. The procedure requires an experimental set-up where the heat conduction equation has a closed analytical or approximate solution explicitly containing the unknown parameters. If this is not possible, a fourth frequently applied method for parameter estimation, the non-linear regression method, seeks to minimize a sum-of-squares error function.

So far, our work on parameter estimation in connection with experiments with the ignitability apparatus has been largely focused on the two last mentioned methods. The efforts to determine material properties k and ρc by non-linear regression (also called non-linear least squares or non-linear estimation) met with mixed success. Very briefly, the methodology was the following: A numerical model gave the temperature-time curves of the exposed surface and the surface between specimen and baseboard for specified values of k and ρc. The model was built on a discretized space coordinate, transforming Eq. 2 into a system of ordinary differential equations, which were solved by using a variant of the Runge-Kutta method. Curves 3 and 7 in Fig. 3 was calculated by this method. The accuracy of the computer program was checked by comparing output to results obtained by a well-known standard program /19/. A standard library routine /18/ was used to determine the property values of k and ρc which in a least squares sense mini-

mized the difference between the numerical model and the experiment.

The conclusions of using non-linear regression can be summarized as follows: Optimization with respect to surface temperatures in some cases gave values of k and ρc different from those obtained when using temperatures from the interface specimen - baseboard. Convergence could be painfully slow and sometimes the algorithm failed. As we were interested basically in obtaining property values describing the surface heating, effort was concentrated on using the experimental surface temperature curves. This led to a new complication in that independent estimation of k and ρc cannot be obtained for a semi-infinite body with only one sensor at x = 0, see e.g. /20/. This follows also directly from considering Eqs. 6, 7 and 10 where k and ρc do not appear isolated but only combined as kρc. The practical implication is that the duration of the experiments must be long enough that the finite thickness of the specimen has an influence on the surface temperature curve. Fig. 4 illustrates for material 1 how the error function varies with values of k and ρc. Also shown is a contour map indicating points where the sum of squares (the error-function) have equal values. The figure shows that convergence towards the point of minimum is very slow.

As a temporary solution and until the optimization procedure had been further investigated it was decided to use Eqs. 10-11 to estimate kρc. It was found that kρc will vary with time (which strictly speaking invalidates the theory behind Eqs. 10-11) but not excessively. Typical examples are given in Fig.

5. The evaluation must be so short that the assumption of semi-infinite specimen thickness is valid. The average values of $k\rho c$ used in subsequent calculations are given by Table 3.

A third approach was also used. The surface temperature rise θ_s of a specimen with known value of $(k\rho c)_0$ was recorded. The corresponding time curve for the material with unknown value of $(k\rho c)_1$ then gives the value of $(k\rho c)_1$ from the condition that for a specific temperature rise θ_s obtained of times t_0 and t_1 respectively

$$\frac{t_0}{(k\rho c)_0} = \frac{t_1}{(k\rho c)_1} \qquad (12)$$

This scaling criteria follows automatically from Eq. 10 (and Eqs. 6 and 7). The values of $k\rho c$ obtained in this way were compatible with the values shown in Table 3.

RHR-MEASUREMENTS

Test equipment

The thirteen materials have been tested in three different RHR-apparatus: The OSU-apparatus /5/, and open configuration /7/ based on a design originally developed of NBS /6/, and the cone calorimeter /8/. The analysis made in this report will be based on the measurements reported in /7/.

The equipment consists of a vertical sample holder and an electrical radiation panel placed under an open hood, see Fig. 6. The radiation intensities can be varied up to 5 W/cm^2.

The different intensities are obtained by varying the distance between the radiation panel and the sample. The sample holder is placed on a balance. A pre-mixed pilot flame above the sample has its base 10 mm behind the sample surface and is directed out from the sample. The oxygen concentration in the exhaust duct is measured by a high temperature zirconium cell, the gas flow by an averaging pressure tube flow meter and the gas temperature by a thermocouple.

All samples were 15 x 15 cm^2 and conditioned at 50% relative humidity and 23°C before testing. The moisture content was determined by drying at 103°C to constant weight.

An noncombustible board (Vermite, 10 mm thick, 700 kg/m^3) served as backing material. The samples were tested at 5, 3 and 2 W/cm^2 and some easily ignitable materials also at 1 W/cm^2. Three examples of test output are given in Figs. 7 a-c for materials 3, 7 and 8, c.f. Table 1.

Background

It has been demonstrated /21/ that modelling of the fire growth can be done based on direct use of the RHR-curves. Nevertheless, a better insight should be gained by breaking down the energy release $\dot{Q}''$ into component parameters.

Formally, the mass loss rate $\dot{m}''_b$ from a burning surface may be written

$$\dot{m}''_b = \frac{1}{L} \dot{q}''_{net} \qquad (13)$$

where $\dot{q}''_{net}$ is the difference between heat flux to the fuel surface (externally applied flux, flux from flames) and heat loss terms (radiative and convective loss from the surface, heat conducted into the bulk of the fuel, cooling agents applied). L may be defined as the heat required to produce volatiles. If we accept Eq. 13 in a formal sense, then $\dot{Q}''$ is given by

$$\dot{Q}'' = \chi \Delta H \dot{m}''_b = \chi \frac{\Delta H}{L} \dot{q}''_{net} \qquad (14)$$

where χ stands for degree of combustion completeness. Obviously, the quantity $\Delta H/L$ is a parameter of major importance. It is also a component in the mass transfer number B, which plays a fundamental role in the theory of convection controlled combustion. An engineering approximation to B is given by the expression

$$B = \frac{\Delta H}{L} r_{ox} Y_{o,a} \qquad (15)$$

where r_{ox} = mass oxygen to fuel stoichiometric ratio and $Y_{o,a}$ = ambient mass fraction of oxygen.

Another use of r_{ox} is involved in the concept of "excess pyrolyzate" and the dimensionless r-number, usually called the mass consumption number /22/. It is the ratio of available oxygen to fuel concentration divided by the stoichiometric oxygen to fuel mass ratio. Large values denote small flame heights, and small values, i.e. insufficient oxygen, denote large flame heights. The r-number can be calculated *a priori* for a specified fluid dynamics situation and used to calculate

the flame height (for a laminar, non-radiation environment). Although scaling relationships have not been established, it can be seen as a comparative measure of hazard in itself. It should be an important parameter in the ceiling fire spread process. Examples of derived r-values are given in /23/.

ΔH and r_{ox} can, at least in theory, be acquired in any RHR-apparatus capable of providing measurements of oxygen consumption, specimen weight loss and mass flow rate through the apparatus. The burning process of the test specimen must not be under-ventilated. The equations are given in /10/. Determination of L is considerably more complicated and open to discussion, especially in the case of charring solids or solids treated with fire retardants. Conventionally, L is measured by employing TGA-techniques. In /23/ L is measured in pyrolysis experiments (heating in inert environments) and a steady-state surface heat balance used to determine L. Transient effects like heat flow into the non-vaporized solid and through a charring layer is neglected. If L (or more precisely 1/L) is determined in actual combustion experiments, expressing mass burning rate as a function of impressed flux, further complexities are added when determining effective heat flux to the surface and surface reradiation.

The initial attempt was to try to derive the parameters ΔH, L and r_{ox} from the RHR-curves examplified by Fig. 7. Unfortunately, it turned out that transient effects (the bulk heating term) made calculation of L unreliable. The longer heating-up period before ignition at lower flux levels in some cases nearly neutralizes the the effect of higher levels of

external flux on rate of mass loss. Regarding ΔH and r_{ox}, which are coupled by the equation

$$\Delta H = r_{ox} \Delta H_{ox} \qquad (16)$$

with ΔH_{ox} approximately = 13.1 kJ/g O_2, they have to be computed on the basis of the experimental weight loss curves. Probably due to the vaporization of moisture the true instantaneous weight loss rate of solid material could not be determined with adequate accuracy. For the same lining material, r_{ox}-values for different levels of impressed heat flux in some cases showed a significant scatter. As a consequence, it was decided to describe and make use of the RHR-characteristics of the involved material directly using a mathematical approximation of the curves shown in Fig. 7, primarily the curves valid for an external flux = 30 kW/m². In the full scale experiments, heat fluxes to the lining material will vary considerably with time and location. A study of available literature indicated that an average value of 30 kW/m² might be more representative than 50 kW/m² but this has not been substantiated.

The experimental curves were idealized in the following way, see Fig. 8. After exposure at t = 0 the sample will gradually heat up and reach pyrolysis temperature T_p at $t = t_p$. The mass loss rate during this period is neglected. At $t = t_p$, pyrolysis and rate of heat release jump to a maximum value $\dot{q}''_{max}$ and start to decay. Asymptotically, the rate of pyrolysis is proportional to $(t - t_p)^{-1/2}$ /24/. For the initial, transient period, which is of the main interest for

room fire growth process, it was found suitable to write

$$\dot{Q}''(t) = \dot{Q}''_{max}\, e^{-\lambda(t-t_p)} \qquad (17a)$$

or, alternatively,

$$\dot{Q}''(t) = \dot{Q}''_{o} + (\dot{Q}''_{max} - \dot{Q}''_{o})e^{-\lambda(t-t_p)} \qquad (17b)$$

Here we will exclusively use Eq. 17a. The $\dot{Q}''_{max}$-values were taken directly from measurement and can be found together with the corresponding regression values of λ in Table 3. Fig. 9 shows experimental curves and approximations according to Eq. 17a for materials 3, 7 and 8.

For the products investigated in this project, with the exception of materials 9 and 10, the expression 17a seemed phenomenologically correct. Thermoplastics like polystyrene which melt and drips away before and after ignition, behave in such a way that modelling seems a remote possibility. Indeed, the room test was at least partly motivated by the incapability of small scale tests to rationally evaluate the flammability characteristics of these materials. For material 9, which is a composite, the general appearance of the small scale test RHR-curves varies with level of impressed flux, with the 30 kW/m²-level producing a RHR-curve increasing in time and the 50 kW/m²-level a decreasing curve. The remaining products may be characterized as char-forming cellulosic materials, in some cases with a thin surface cover. A more detailed presentation is given in /7/.

FULL SCALE TEST

The full scale test room /9/, built at the Swedish National Testing Institute is a lightweight concrete construction with dimensions according to the proposed ASTM standard room fire test /25/. Rate of heat release is measured by the oxygen consumption method. For the room tests the paramagnetic oxygen analyzer has proved to be the only useable instrument. The test room has been extensively calibrated with results indicating that the total inaccuracy of the system is within 25 kW or $\pm$10% of the measured value. In the full scale test series the material was mounted on the ceiling and all walls except the doorway wall. The material was ignited with a 0.17 m square propane sand burner located in one corner of the test room. During the first 10 minutes of an experiment the gas burner heat output was kept at 100 kW, which produced a flame that reached the ceiling. If flashover had not occurred the heat output was then increased to 300 kW and the experiment was discontinued after another 10 minutes.

METHODS OF ANALYSIS

What has been presented so far is a small percentage of the data available. When analysing the full data set, several methodologies are possible. These include a statistical factor analysis, a statistical modelling of the full scale test process using regression analysis, deterministic modelling using the zone-volume approach, the field equation methodology, scale modelling, etc. We will here concentrate on the second method, leave others to future reports and only mention that

the zone-modelling efforts will be based on the computer program described in /21/.

The different approaches reflect the degree of knowledge we have of the physical processes. The factor analysis method is of the "black box" type; typical discrete events in the fire growth (time to 500 kW, time to flashover, etc) are described as a function of the independent variables such as ignition source output and kρc of lining material. Nothing is assumed known of the fire growth phenomenon. The second method assumes that the basic structure of the model is understood and that unknown parameters in the model can be estimated by regression analysis. Deterministic zone-modelling requires a more detailed knowledge of component processes, etc.

The reason for concentrating the initial efforts on statistical regression analysis is that this procedure promises to be the fastest way of obtaining a design equation or design procedure; albeit they may be approximate and temporary ones.

REGRESSION ANALYSIS

Basic model structure

The scenario we are considering is the following one: The walls and the ceiling of the test room are lined with the material, the ignition source in the corner ignites the wall corner material and rapidly spreads upward on an area approximately = 0.7 m^2 equal to the width of burner (0.17 m) times distance burner - ceiling. The resulting ceiling jet or flame

spreads along the intersections walls - ceiling and along the ceiling area in the mode of concurrent flame propagation. The model is primarily intended to describe this phase of the fire growth. After a certain time delay, flames begin to spread vertically downward from the ceiling and horizontally from the burning corner plume area. The mode of the flame spread is here "creeping" or opposite the air flow direction.

Our model will be based on the concepts presented in /26/, /27/ and /28/. It is demonstrated in these that for the ceiling flow

* flame area is linearly increasing with the total rate of heat production, i.e. with the pyrolysis area A_p

* subsequent pyrolysis areas A_p are proportional to the initial pyrolyzing area $A_{p,o}$

* the rate of spread of A_p is inversely proportional to the time Δt necessary to increase the surface temperature at the flame tip from an initial temperature T_i to a pyrolysis temperature T_p.

The total rate of heat release $\dot{Q}_{F,t}$ at time $\approx t_b$ may be written as the product of A_p and a time-averaged value of $\dot{Q}''(t)$

$$\dot{Q}_{F,t} = A_p \, \dot{Q}''(t_{av}) \qquad (18a)$$

with $0 \leq t_{av} \leq t_b$ and as yet undetermined.

From the results enumerated above it follows that A_p may be considered as a driving force in a process where the rate of increase of A_p is proportional to the quantity A_p itself; i.e. A_p is exponertially increasing with time. For the quantity Δt and a thermally thick material

$$\Delta t \sim k\rho c(T_{ig} - T_a)^2/\dot{q}''^2 \qquad (18b)$$

where effective heat flux $\dot{q}''$ may be formally written

$$\dot{q}'' = h(T_f - T_s) \qquad (18c)$$

with h = total heat transfer coefficient.

It follows that A_p ca be written in a general sense as

$$A_p = f(e^{h^2 t/k\rho c}) \qquad (18d)$$

and that it is natural that a regression equation for the rate of heat release $\dot{Q}$ in the room test is written in the following form

$$\dot{Q}_{rt}(t) = \alpha(e^{h^2 t/k\rho c} - 1)^{\beta}\ \dot{Q}''(t_{av}) \qquad (18e)$$

where α and β are coefficients to be determined and where t_{av} is the time to evaluate an average value of $\dot{Q}''$ from the small scale rate of heat release test (see Eq. 17a). If we look at the interaction between flame spread and rate of heat release, see Fig. 11, the correct method of calculating the

value of $\dot{Q}_{rt}$ should be to use a superposition, Duhamel type integral /29/. If we apply this method to our model and data we obtain a simple expression for the integral, see Fig. 11. We have

$$\dot{Q}'' \sim e^{-\lambda t} \tag{19a}$$

$$A_p \sim e^{at} \quad \text{with } a = h^2/k\rho c \tag{19b}$$

$$\Delta A_p \sim a\ e^{at}\ \Delta t \tag{19c}$$

For the infinitesimal area $\Delta A_{p,k}$ at time step k

$$\dot{Q}'' = \dot{Q}''(t_b - k\Delta t) = \dot{Q}''_{max}\ e^{-\lambda(t_b - k\Delta t)} \tag{20}$$

and for the total pyrolyzing area A_p

$$\dot{Q}_{rt} \sim \int_0^{t_b} a\ e^{a\tau} \dot{Q}''_{max}\ e^{-\lambda(t_b - \tau)} d\tau = \dot{Q}''_{max}\ \frac{a}{a+\lambda}\ (e^{at_b} - e^{-\lambda t_b}) \tag{21}$$

Eq. 21 is a direct physical interpretation of the so called Duhamel's formulas expressing the response of a system to a general driving function $A_p(t)$ in terms of the experimentally accessible response ($\dot{Q}''(t)$ from Eq. 17) of the system to a unit step function /32/. The methodology can be expanded to treat the case where the step response $\dot{Q}''(t)$ is a function of impressed flux instead of being linked to the constant value 30 kW/m². It has previously been used to correct heat release measurements from various small scale test apparatuses for the effect of inherent time delays in the measurement system /33/, /34/, /35/.

Grouping of materials

Looking at the full scale tests, it was decided to divide the materials into two groups: one for which the depth of combustible material was thick enough so that no burning through would occur during time up to flashover (materials 1, 2, 3, 9, 11, 12, 13), the other for which a thin combustible surface finish covered an incombustible baseboard (materials 4, 5, 6, 7, 8). Material 10, polystyrene, was left outside the analysis. The full scale effect release curves for materials 3, 7 and 8 are shown in Fig. 10.

Starting procedure

From Fig. 10 it is clear that the system may have a substantial and varying time-lag during the starting period of the experiments. It is essential that the regression equations are applied to a process with a well defined starting point. For this reason we define the quantity $\dot{Q}_{start}$ as follows: The original flame, which starts pyrolyzing the ceiling material and determines the subsequent spread, can be seen to be composed of combustibles from three sources: fuel from the burner + fuel from the 0.7 m² wall corner plume - fuel consumed in the wall corner flame. We call the sum of the first two parts for $\dot{Q}_{start}$ and the effect that can be released in the ceiling flame for $\dot{Q}_{ef}$. If the burner is turned on at t = 0 a certain time t_{start} will elapse before the instruments register $\dot{Q}_{start}$. The time-lag will have a number of components: ignition delay of wall corner material, filling time

of the room, transport time to oxygen measurement system, instrument time. It is clear that some of these will vary with flammability characteristics of the tested material.

In order to arrive at a practicable expression for t_{start} a study was made of the correlation between t_{start} and the ignitability of the materials. The result was Fig. 12. It can be seen that with one exception, material 13, t_{start} is closely approximated by the equation

$$t_{start} = t_{ig} + 5 \qquad (s) \qquad (22)$$

with t_{ig} measured at the 30 kW level.

Again, alternative procedures to describe the effect of the time lag inherent in the ignition process and in the transport and measurement system are available. The response of the test room to a unit step load (gas-burner with known effect) has been determined and makes it possible to utilize the superposition method described earlier and in references /33-35/. For the moment, we assume that the simple time-delay expression given by Eq. 22 is valid. We then arrive at the following regression equation for $\dot{Q}_{rt}$, replacing Eq. 18e

$$\frac{\dot{Q}_{rt} - \dot{Q}_{start}}{\dot{Q}_{cf}} = \alpha(e^{at} - 1)^{\beta} \cdot \dot{Q}''(t_{av}) \qquad (23a)$$

or

$$\frac{\dot{Q}_{rt} - \dot{Q}_{start}}{\dot{Q}_{cf}} = \alpha(e^{at} - e^{-\lambda t})^{\beta} \cdot \dot{Q}''_{max} \cdot \frac{\alpha}{\alpha\ \lambda} \qquad (23b)$$

replacing Eq. 21.

It should be observed that time t in Eqs. 23 will be measured from $t = t_{wstart}$.

It remains to determine $\dot{Q}_{cf} = \dot{Q}_{wstart}$ - wall flame combustion. A study of air entrainment into the wall plume according to /30/ showed that approximately 30 g O_2/s corresponding to a heat release of 400 kW , is entrained into the wall flame. It is reasonable to assume that actual combustion before the plume hits the ceiling may be in the area of 60-150 kW. As the computations will be insensitive to choice of $\dot{Q}_{cf}$, mainly changing the value of the parameter α with a constant, it was decided to arbitrarily put

$$\dot{Q}_{cf} = \dot{Q}_{wstart} - 60 \qquad (24)$$

Results of parameter estimation

If the logarithm is taken of both sides of Eq. 23, the relations are transformed into first-order linear models where the parameters α' ($= \ln\alpha$) and β can be determined by linear regression. With $\dot{Q}_{rt}$ describing the output from the full scale tests, this procedure was followed for the seven materials 1, 2, 3, 9, 11, 12 and 13, using a standard library regression programme /31/. When using Eq. 23a, the value of t_{av}, c.f. Eq. 18a, must be selected. The computer runs showed that the variation in flame area e^{at} had such an impact compared to the variation in $\dot{Q}''(t)$ that the method of choosing t_{av} was not crucial. This can also be seen in Table 4

which gives the value of α' and β plus the correlation coefficient r for the seven materials, using Eqs. 23a and b as a base. In Eq. 23a, $t_{av} = t/2$. Computations with $t_{av} = t/4$ gave very similar results. The value of t_{start} was in each individual case taken directly from the full scale measurements, not from Fig. 12. The value of the heat transfer coefficient h from ceiling flame or jet to lining material must be specified. As an initial approximation, a constant average value of 40 W/m^2 K was considered reasonable.

As can be observed, the regression model points to negligible difference between Eq. 23a and Eq. 23b. Consequently, for the remaining part of this paper we will concentrate further computations on Eq. 23a. It should be remembered, however, that in Table 4 heat release rate is linked to a single curve for each material. A more correct model taking into account that impressed flux is variable during the full scale experiments may indicate the need for choosing rate of heat release characteristics more realistically.

The outputs of a general least square computer programme usually includes standard error of the undetermined coefficients, standard error of the dependent variable, an analysis of the variance table and the value of the (multiple) correlation coefficient r. A closer study of the computed residuals and confidence bounds have not been carried out as yet, but the values of correlation coefficient r in Table 4 indicate that the models of Eq. 23 are reasonable. At the same time, there is a variaton in α' and especially β between the materials which could invalidate use of Eq. 23a in a design model.

For this equation to be generally applicable for design purposes, variations in α' and β must have a limited influence on the final results. The next section will deal with this question.

Accuracy of prediction model

For the model according to Eq. 23a the average values and coefficients of variation for α' and β are

$$\overline{\alpha}' = -4.58 \qquad (24a)$$

$$\sigma_{\alpha'}/\overline{\alpha}' = 0.13 \qquad (24b)$$

$$\overline{\beta} = 1.15 \qquad (25a)$$

$$\sigma_{\beta}/\overline{\beta} = 0.276 \qquad (25b)$$

Seen in the light of the scatter inherent even in standard small scale fire tests, the variability does not seem excessive. To find out its practical importance, the full scale tests were recalculated on the basis of the values of α' and β given by expression 24a and 25a, i.e. the average values. Furthermore, t_{start} was determined by Eq. 22. Evidently this procedure is something of a circle proof that had to be accepted for lack of independent experimental data. The results can be seen in Figs. 13a-g. In substance, the agreement indicated the general validity of the derived parameters α and β. There are two essential deviations: material 9, which behaved erratically in the small scale tests /11/, and material 13. Here the

difference is due to the fact that material 13 takes much longer to ignite in the small scale test than in the full scale one, see Fig. 12. A recalculation using the correct ignition time for the room experiment showed a considerably better agreement, see Fig. 13g.

Thin surface finishes on non-combustible baseboard

Five materials, No. 4, 5, 6, 7 and 8, can be regarded as thin combustible surface finishes on non-combustible baseboard. In only one case, material 8, was there a flashover during the initial period of 10 minutes with burner output = 100 kW. If we rewrite Eq. 23a and replace t_{mv} with t we get

$$\dot{Q}_{rt} = \dot{Q}_{start} + \dot{Q}_{cf} \cdot \alpha \cdot (e^{at} - 1)^{\beta} \cdot \dot{Q}''_{max}\, e^{-\lambda t} \qquad (23')$$

This expression will be bounded for all t only if

$$\beta a < \lambda \qquad (26)$$

A look at Table 3 reveals that the condition is approximately fulfilled for materials 4, 5, 6 and 7 but decidedly not for material 8. The ratio $\beta a/\lambda$ is approximately 1.0, 0.72, 0.77, 0.72 and 9.7 for the five materials.

Eq. 26 expresses the unbalance between the two competing processes: flame growth and decay in heat release rate. It is probably too crude to be used as a design formula in its present shape but may serve as a guide for further research.

Finally, an effort was made to numerically simulate the room test for material B, where flames extended over half the ceiling after about 90 seconds but then subsided, c.f. Fig. 10. In reference /28/ it is demonstrated that flame area A_f in the ASTM E84 test is proportional to heat release $\dot{Q}$

$$A_f = f \cdot \dot{Q} \qquad (27)$$

with f approximately = 0.022 m^2/kW.

Using the assumption that f could be approximately the same in the room test, experiment 7 was numerically simulated. The results can be seen in Fig. 14. The results are sensitive to choice of $\dot{Q}_{cf}$ and f and should at this stage more be seen as computational exercises. All the same, the results implicate that a rational calculation procedure may be possible.

Summary of calculation procedure

Before making comments on the results obtained so far, it may be appropriate to repeat the various steps which have been taken in the calculation procedure.

1. For a specified lining material, determine a value of $k\rho c$ and time to ignition at 30 kW/m^2.

2. Calibrate the test room with respect to time-lag in heat effect measurement system, c.f. Eq. 22.

3. Derive values of $\dot{Q}''_{max}$ and the decay factor λ.

4. Calculate the values of $\dot{Q}_{start}$ and $\dot{Q}_{ef}$ using the definition of $\dot{Q}_{start}$ and Eq. 24.

5. Put h = 40 W/m^2 K.

6. Put $\alpha' = \overline{\alpha'}$ and $\beta = \overline{\beta}$, according to Eqs. 24a and 25a. Observe that $\alpha' \approx \ln(\alpha)$.

7. Use Eq. 23a to derive time curve $\dot{Q}_{rt}$ of heat output from room test.

REMARKS ON THE RESULTS

No sensitivity testing has so far been carried out with respect to the different assumptions and procedures enumerated above. It is most likely that substantial changes can be introduced into the analysis, leading to an improved consistency. As an example, putting the heat transfer coefficient equal to a constant is an oversimplification. It should be possible to describe h as a function of $\dot{Q}_{rt}(t)$ and in this way lessen the tendency of Eq. 23a to underestimate $\dot{Q}_{rt}(t)$ when the test process is approaching flashover. Also the effect of the mass consumption number r should be investigated.

Likewise, it should be investigated how various assumptions regarding the calculation of $\dot{Q}_{ef}$ influences the final result. The starting time for the regression analysis $t_{\dot{Q}_{start}}$ probably varies with the RHR-characteristics of the lining materials.

A number of laboratories are operating the ASTM/ISO full scale room fire test, and most of them have access to the ignitability and RHR test methods. In a short time, there should exist a data base which permits a correct statistical evaluation of safety factors. These will probably be derived on the basis of the variability and the irregularity the lining material has exhibited in the small scale tests. It will be necessary to standardize the experimental and data extraction procedures employed to produce values of $k\rho c$, $\dot{Q}''_{max}$ and λ. Possibly they should be automatic and on-line and an optional part of the test standard.

Finally, it should be pointed out that even if the predictive capability of the analysis in a quantitative sense may still be limited, it can be used qualitatively to rank materials. If we rank the seven materials with respect to the time it takes for the fire room test to reach 1 MW, the relative ranking is coincident in experiment and design theory. See Table 5.

In summary, it is thought that a first step has been taken in the efforts to use results from small scale flammability tests to rationally predict full scale fire growth (for one specified scenario) and rank materials. Further efforts should be directed firstly towards other fire scenarios, secondly towards code calibration studies. The sensitivity studies needed to derive confidence regions and safety factors can be based on the first order, second moment statistical methods used in /38/ in the area of structural fire endurance.

ACKNOWLEDGEMENT

The authors want to thank the other members of the project group for their valuable reviews. Berit Andersson is additionally thanked for her help in doing much of the computational work.

REFERENCES

/1/ Pettersson, O., "Fire Hazard and the Compartment Fire Growth Process - Outline of a Swedish Joint Research Program", FoU-brand, No. 1, 1980. Department of Structural Mechanics, Lund Institute of Technology, Report R80-5, 1980.

/2/ Östman, B., "Ignitability as Proposed by the International Standards Organization Compared with Some European Fire Tests for Building Panels", Fire and Materials, Vol. 5, No. 4, 1981.

/3/ ISO DTR 5658, "Fire Test Reaction to Fire - Spread of Flame of Building Materials", ISO/TC92/SC1 N88, Oct. 1982.

/4/ Robertson, A., "A New Fire Test for Surface Flammability", International Maritime Organization (IMO) FP/332, Dec. 1982.

/5/ Blomqvist, J., "RHR of Building Materials - Experiments

with and OSU-Apparatus Using Oxygen Consumption", Division of Building Fire Safety and Technology, Lund University, Lund, Report LUTVDG/(TVBB-3017), 1983.

/6/ Sensenig, D.L., "An Oxygen Consumption Method for Determining the Contribution of Interior Wall Finishes to Room Fires", NBS Technical Note 1128, 1980.

/7/ Svensson, G, and östman, B., "Rate of Heat Release by Oxygen Consumption Testing of Building Materials", STFI-Meddelande Serie A Nr 812, Stockholm, Febr., 1983.

/8/ Babrauskas, V. "Development of the Cone Calorimeter - A Bench-Scale Heat Release Rate Apparatus Based on Oxygen Consumption, National Bureau of Standards (US), NBSIR 82-2611, 1982.

/9/ Wickström, U. et al, "The Developement of a Full Scale Room Fire Test", Fire Safety Journal, Vol. 5, 1983, pp 191-197.

/10/ Quintiere, J., "An Assessment of Correlations between Laboratory and Full-Scale Experiments for the FFA Fire Safety Program, Part 2: Rate of Energy Release in Fire", NBSIR 82-2536, July 1982.

/11a/ Quintiere, J., "A Simplified Theory for Generalizing Results from a Radiant Panel Rate of Flame Spread Apparatus", Fire and Materials, Vol. 5, June 1981.

/11b/ Harkleroad, M., Quintiere, J. and Walton, W., "Radiative Ignition and Opposed Flow Flame Spread Measurements in Materials", Report No. DOT/FAA-CT-83/28, U.S. Department of Transportation, FAA Technical Center, Atlantic City Airport, N.J. 08405.

/12/ Heselden, A., "Notes on the Meaning and Use of the ISO Ignitability Test", ISO/TC92/WG2 N33.

/13/ Rasbash, D.J., "Relevance of Fire Point Theory to the Assessment of Fire Behaviour of Combustible Materials", International Symposium Fire Safety of Combustible Materials, Edinburgh, Oct. 1975.

/14/ Ozisik, M.N., "Heat Conduction", John Wiley 1980, p 380.

/15/ Atreya, A., "Pyrolysis, Ignition and Fire Spread on Horizontal Surfaces of Wood", Thesis, Harvard University, May 1983, Appendix E.

/16/ Dubus, J.P. et al, "Méthode Automatique de Caractérisation des Propriétés Thermique d'un Matériau par Identification de la Réponse Indicielle", Annales de l'Institut Technique du Batiment et Travaux Publique, No. 372, France, May 1979.

/17/ Kavianipour, A. and Beck, J.V., "Thermal Property Estimation Utilizing the Laplace Transform with Application to Asphaltic Pavement", Int. J. Heat Mass Transfer, Vol. 20, 1977, pp 259-267.

/18/ NAGLIB E04 JAF, May 1977.

/19/ Abrahamsson, L., Hägglund, B. and Janzon, K., "HSLAB - An Interactive Program for Onedimensional Heat Flow Problems", FOA C20288-D6(A3), Stockholm, 1979.

/20/ Beck, J.V. and Arnold, K.J., "Parameter Estimation in Engineering Science", John Wiley 1977, p 448.

/21/ Smith, E.E. and Satija, S., "Release Rate Model for Developing Fires", Journal of Heat Transfer, Vol. 105, May 1983, pp 281-287.

/22/ Pagni, P.J: and Shih, T.M., "Excess Pyrolyzate", 16th Symposium (International) on Combustion, The Combustion Institute, Pittsburgh, Pa, 1976, p 1329.

/23/ Tewarson, A., "Physico-Chemical and Combustion/Pyrolysis Properties of Polymeric Materials", FMRC J.I. OEON6.RC, RC80-T-70, Nov. 1980.

/24/ Delichatsios, M.A. and de Ris, J., "An Analytical Model for the Pyrolysis of Charring Materials", presented at the CIB W14 meeting in Borås, Sweden, May 1983.

/25/ "Proposed Method for Room Fire Test of Wall and Ceiling Materials and Assemblies", Annual Book of ASTM Standards, part 18, Nov. 1982.

/26/ Orloff, L., de Ris, J. and Markstein, G.M., "Upward Turbulent Fire Spread and Burning of Fuel Surfaces", 15th Symposium (International) on Combustion, 1975.

/27/ Fernandez-Pello, A.C. and Mao, C.P., "A Unified Analysis of Concurrent Modes of Flame Spread", Combustion Science and Technology, Vol. 26, 1981, pp 147-155.

/28/ Parker, W.J., "An Assessment of Correlations Between Laboratory and Full Scale Experiments for the FAA Aircraft Fire Safety Program, Part 3: ASTM E84", NBSIR 82-2564, Center for Fire Research, Washington DC.

/29/ Wickström, U., "Internal Working Memorandum", Dec. 1983.

/30/ Cetegen, B.M., Zukoski, E.E. and Kubota, T., "Entrainment and Flame Geometry of Fire Plumes", Cal Tech, Aug. 1982.

/31/ P1R-BMDP Biomedical Computer Program, P-series, University of California, LA, 1979.

/32/ Wylie, C.R., "Advanced Engineering Mathematics", McGraw-Hill, 4th Edition, p 313.

/33/ Evans, D.D. and Breden, L.H., "A Numerical Technique to Correct Heat Release Rate Calorimetry Data for Apparatus Time Delay", NBSIR 77-1302, Center for Fire Research, Washington, Nov 1977.

/34/ Vandevelde, P., "An Evaluation of Heat Release Criteria in Reaction-to-Fire Tests", Fire and Materials, Vol. 4, No. 3, 1980.

/35/ Holmstedt, G., "Rate of Heat Release Measurements with the Swedish Box Test", Technical Report SP-RAPP 1981:30, Borås, Sweden.

/36/ The Development of Tests for Measuring "Reaction to Fire" of Building Materials, ISO Technical Report 3814, 1975.

/37/ Fire Hazard and the Design and Use of Fire Tests, ISO Technical Report 6585, 1979.

/38/ Magnusson, S.E., "Probabilistic Analysis of Fire Exposed Steel Structures", Bulletin 27, Division of Structural Mechanics and Concrete Construction, Lund University, 1974.

Table 1 Tested materials

No	Type	Thickness (mm)	Weight	
1	Insulating fibreboard	13	250	kg m^{-3}
2	Medium density fibreboard	12	600	kg m^{-3}
3	Particle board	10	750	kg m^{-3}
4	Gypsum plaster board	13	700	kg m^{-3}
5	PVC wallcovering on gypsum plaster board	0.7	240	g m^{-2}
6	Paper wallcovering on gypsum plaster board	0.6	200	g m^{-2}
7	Textile wallcovering on gypsum plaster board	0.7	370	g m^{-2}
8	Textile wallcovering on mineral wool	50*	100*	kg m^{-3}
9	Melamine faced particle board	1.2	810**	kg m^{-3}
10	Expanded polystyrene	50	20	kg m^{-3}
11	Rigid polyurethane foam	30	30	kg m^{-3}
12	Wood panel, spruce	11	530	kg m^{-3}
13	Paper wallcovering on particle board	see No. 6		

* Refers to mineral wool

** Density of entire product

The wallcoverings were glued on the substrates (similar types as materials Nos. 2-4) according to the manufacturers' instructions. The expanded polystyrene was glued on 10 mm thick calcium silicate board.

Table 2

No	Tested method designation	Ref
1	ISO ignitability	2
2	ISO surface spread of flame	3
3	IMO surface spread of flame	4
4	OSU RHR-apparatus	5
5	STFI-Sensenig RHR-apparatus	6, 7
6	Cone calorimeter	8
7	Swedish box test	
8	NBS smoke density chamber	
9	1/3 model scale room	
10	Full scale room	9

Table 3

Mat No	$k\rho c * 10^{-3}$ $(W/m^2\ K)^2$	$\dot{Q}''_{max}$ (kW/m^2)	λ (s^{-1})
1	41	139.8	0.0070
2	80	162.4	0.0027
3	110	199.8	0.0049
4	100	27.7	0.0150
5	75	107.5	0.0293
6	100	105.3	0.0208
7	80	222.0	0.0278
8	4.3	246.2	0.0382
9	105	40.9	-0.0032
10	-	-	-
11	4.0	130.6	0.0217
12	85	149.7	0.0086
13	110	164.1	0.0035

Table 4

Material	Eq. 23a			Eq. 23b		
	α'	β	r	α'	β	r
1	-4.69	1.77	0.994	-4.78	1.78	0.994
2	-4.13	1.22	0.993	-4.16	1.22	0.993
3	-4.34	1.23	0.983	-4.40	1.23	0.982
9	-5.33	0.79	0.980	-5.52	0.75	0.973
11	-5.14	1.06	0.947	-5.14	1.04	0.944
12	-4.39	0.97	0.962	-4.42	0.93	0.958
13	-3.89	1.02	0.993	-3.91	1.01	0.993

Table 5

Time(s) to reach 1 MW in room test		
Material	Experiment	Design equation
1	66	65
2	140	134
3	165	166
9	499	351
11	14	14
12	139	146
13	148	~205

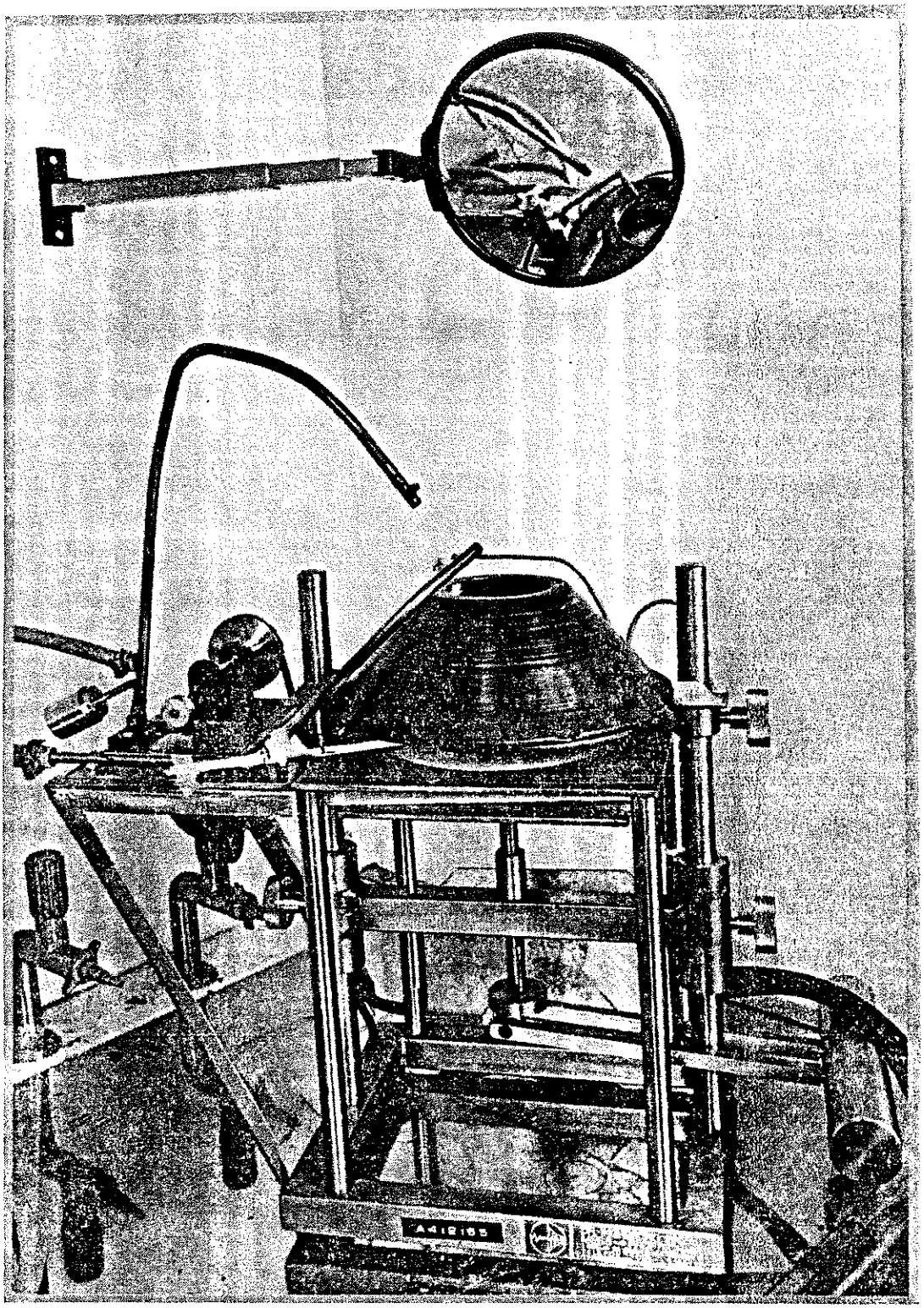

FIG. 1 The ISO ignitability apparatus

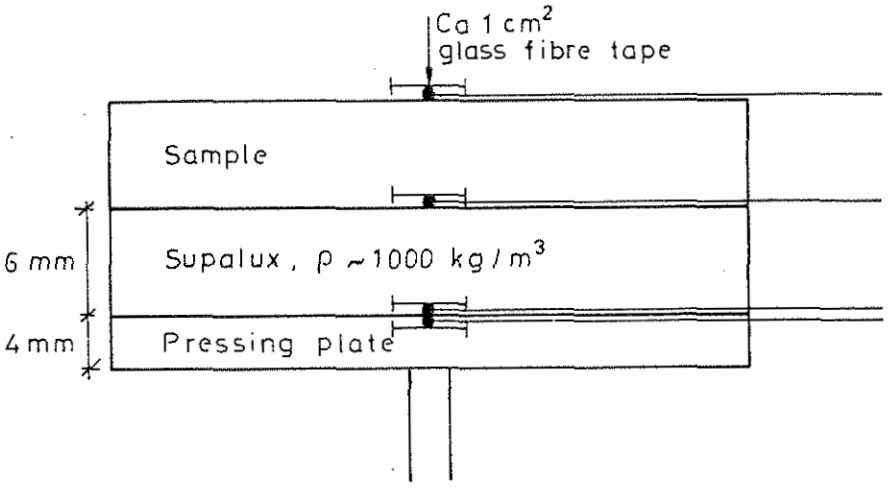

FIG. 2 Sample and temperature measurement system

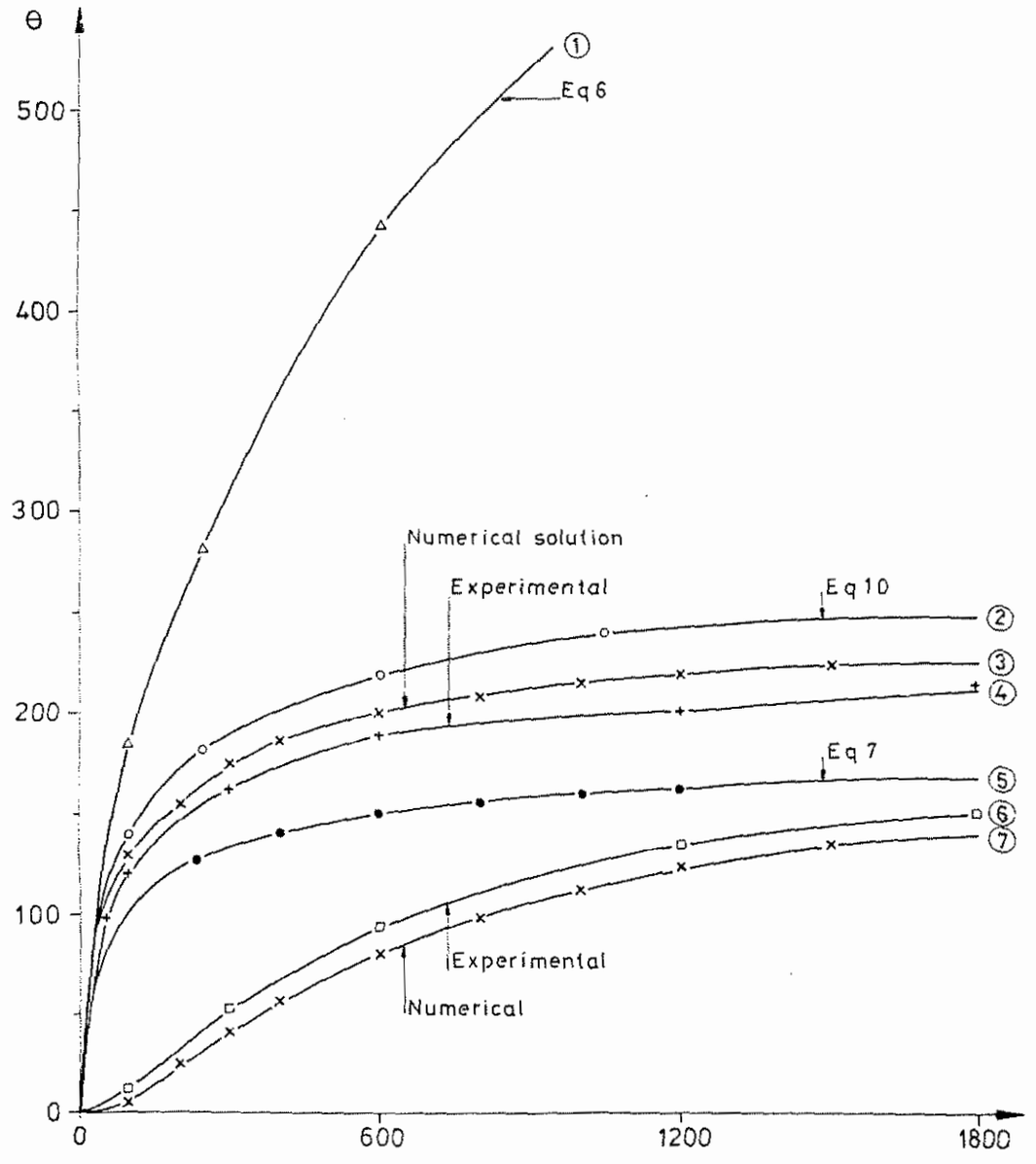

FIG. 3 Temperature curves, calculated and measured

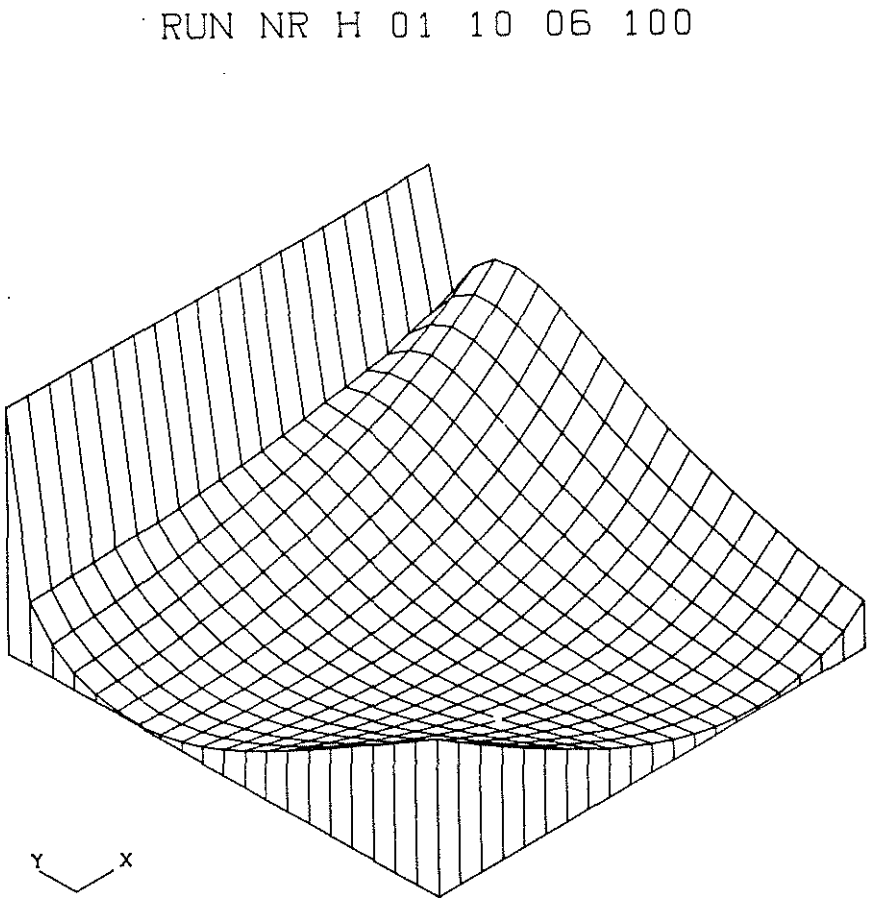

FIG. 4a The variation of error function with thermal conductivity k and thermal capacity ρc for material No. 1 and surface temperature measurement

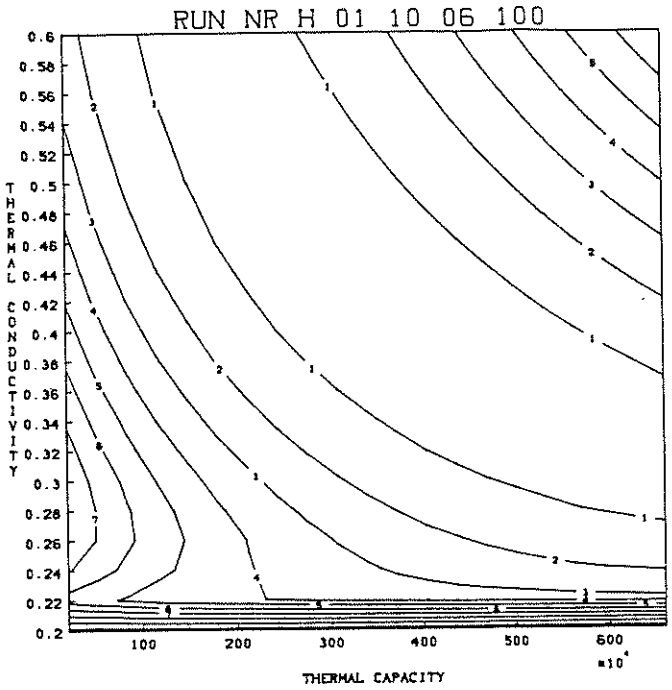

CONTOUR KEY	
1	62.6
2	164.7
3	266.9
4	369.0
5	471.1
6	573.3
7	675.4
8	777.5
9	879.7
10	981.8

FIG. 4b Contour map of Fig. 4a

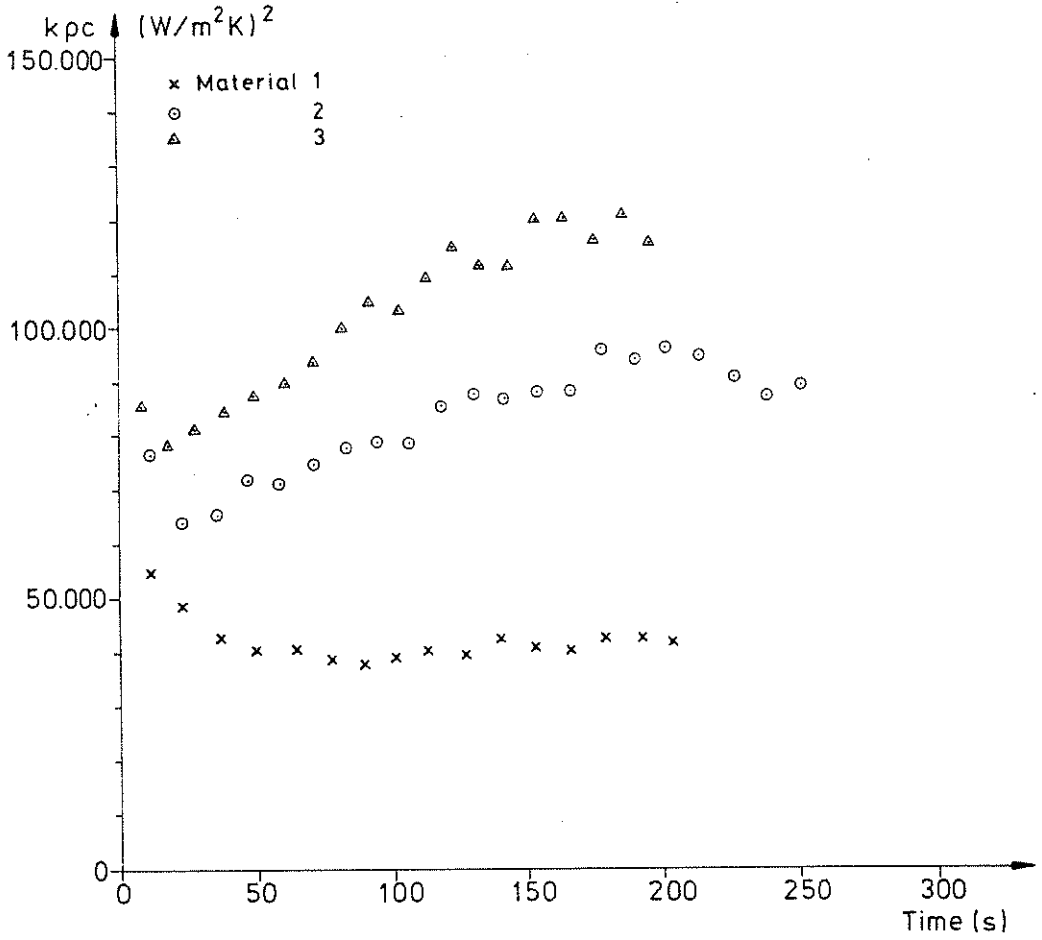

FIG. 5 kρc values obtained from Eq. 10 for three materials

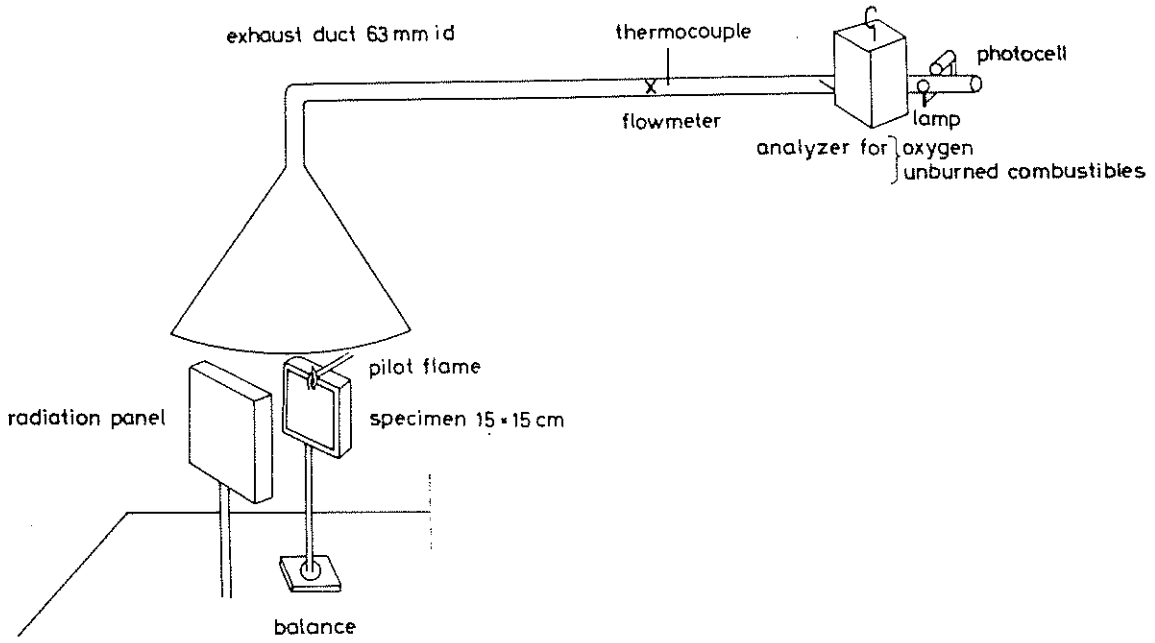

FIG. 6 RHR-apparatus

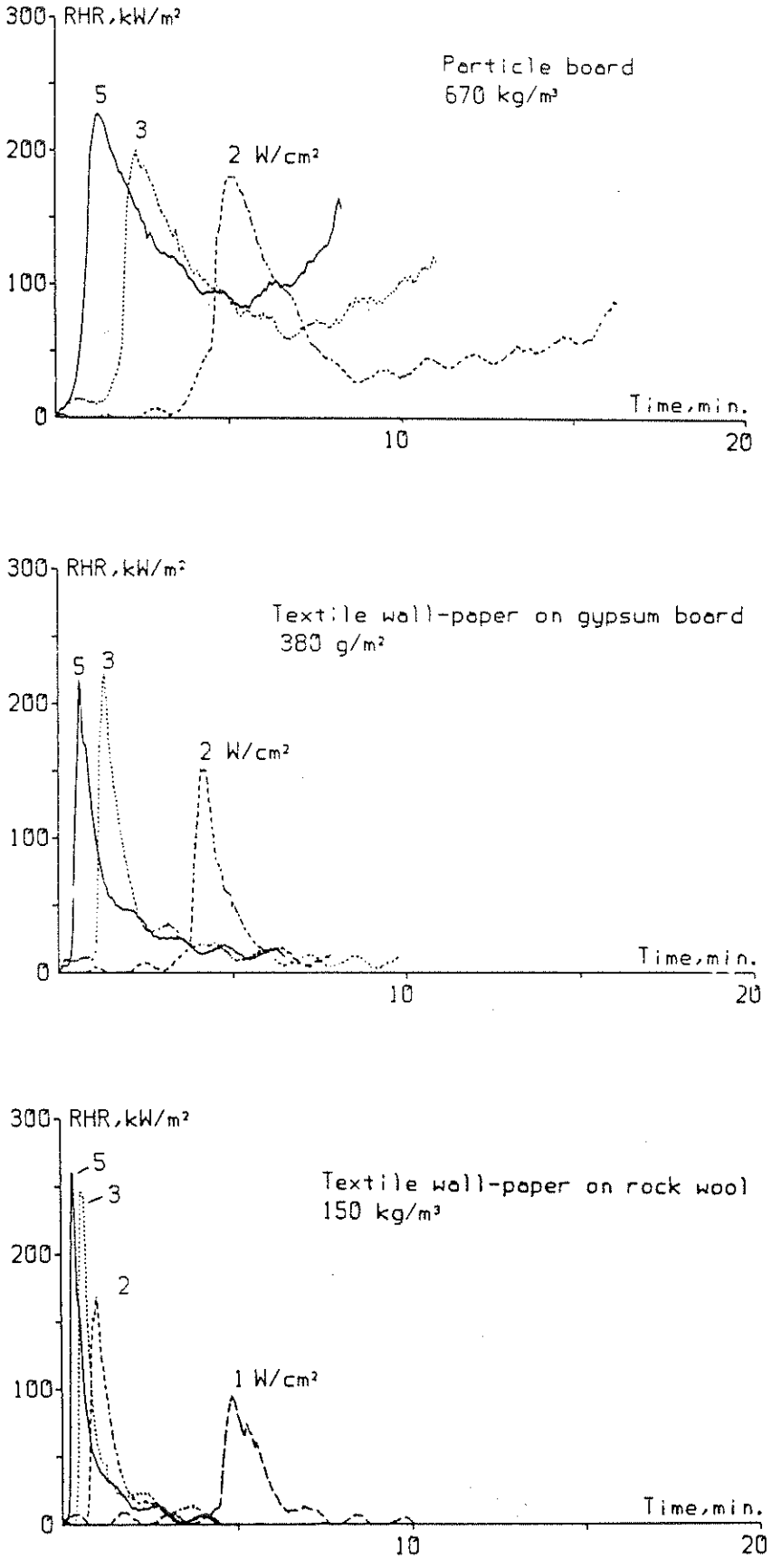

FIG. 7 Experimental RHR curves for material 3, 7 and 8

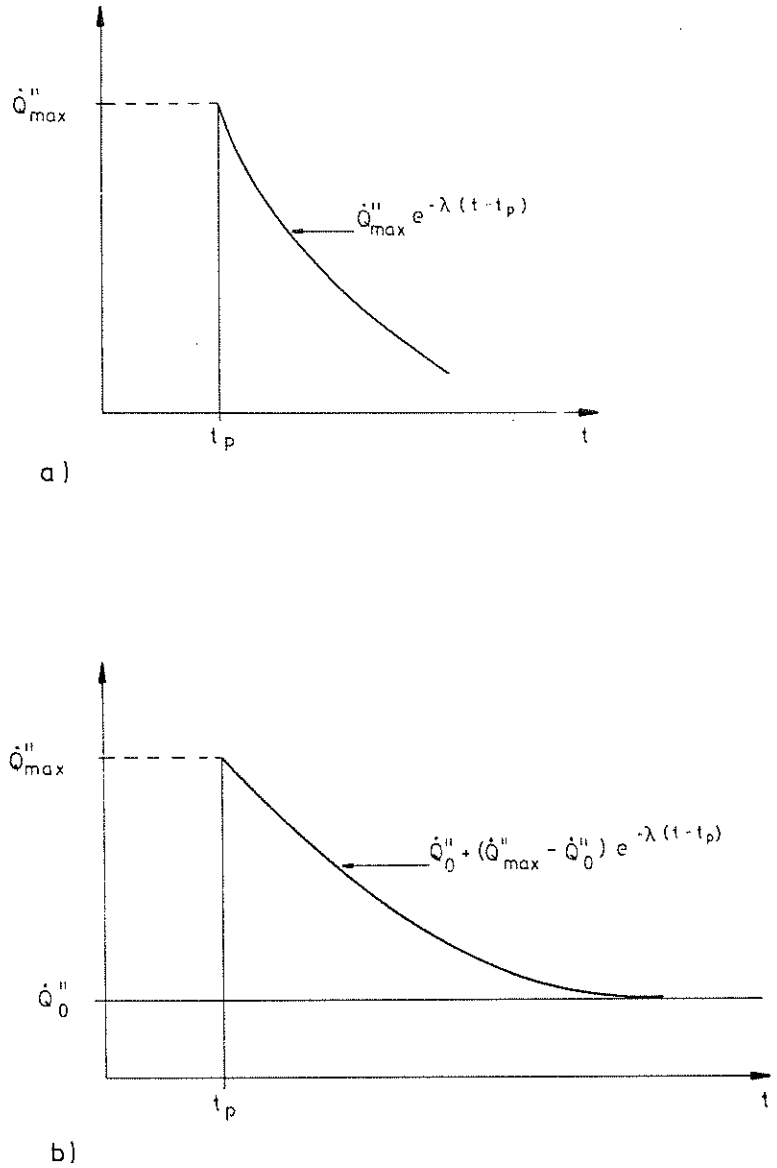

FIG. 8 Principle for analytical approximation of experimental RHR curves

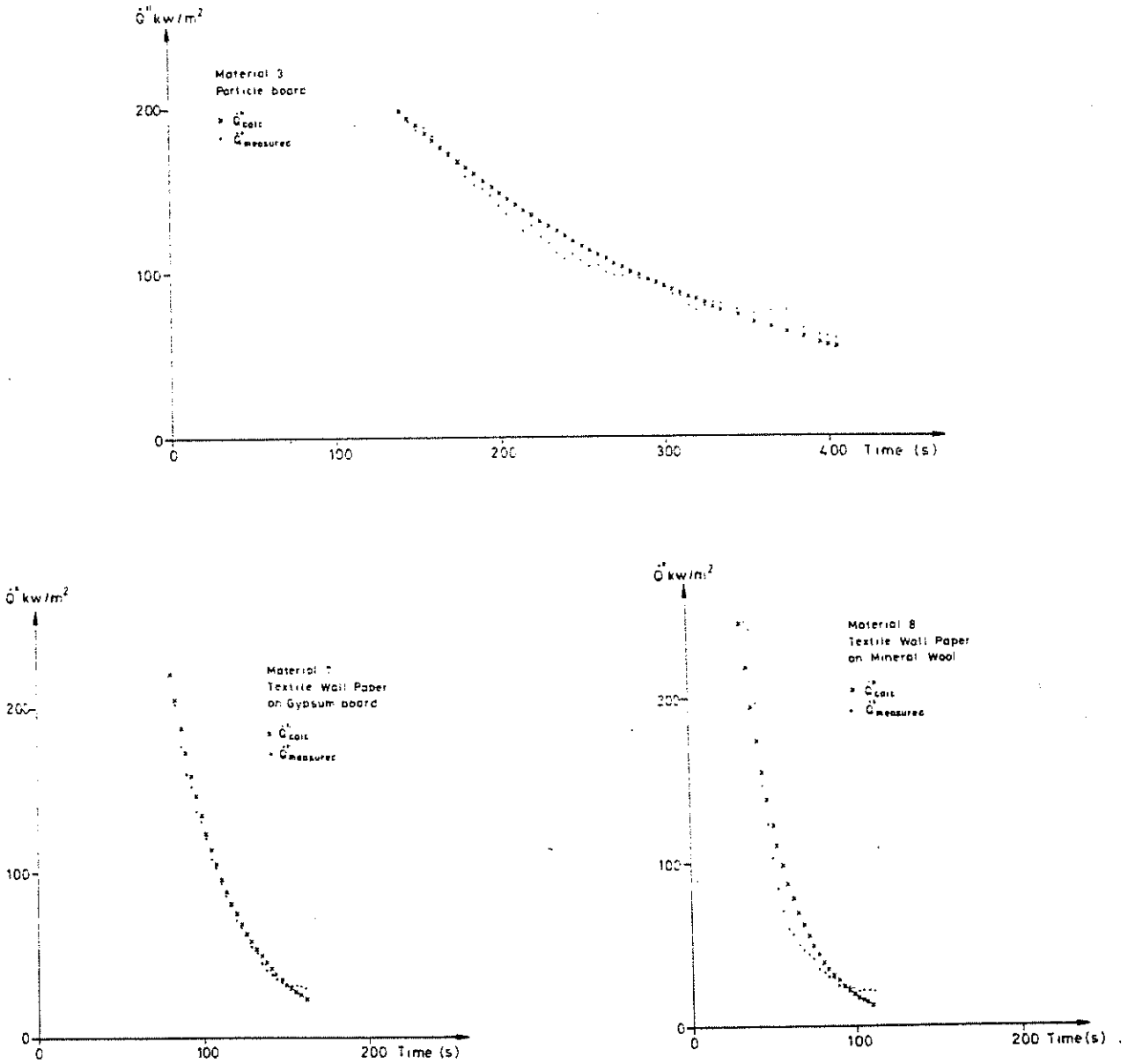

FIG. 9 Experimental RHR curves and the corresponding analytical approximation Eq. 17a

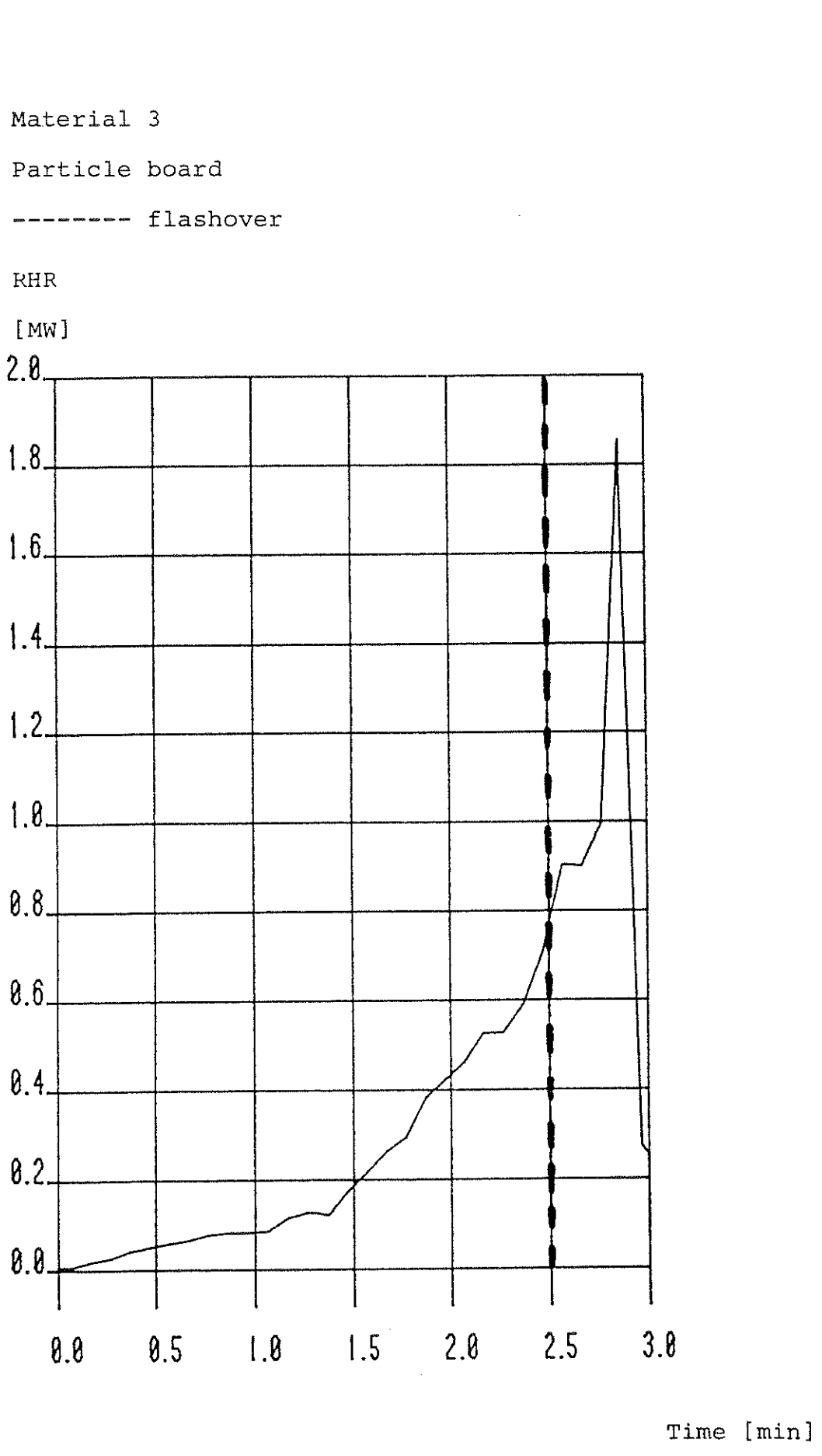

FIG. 10 Experimental heat output curve for full scale room test with material 3

Material 7

Textile wallcovering on gypsum plaster board

------- flashover

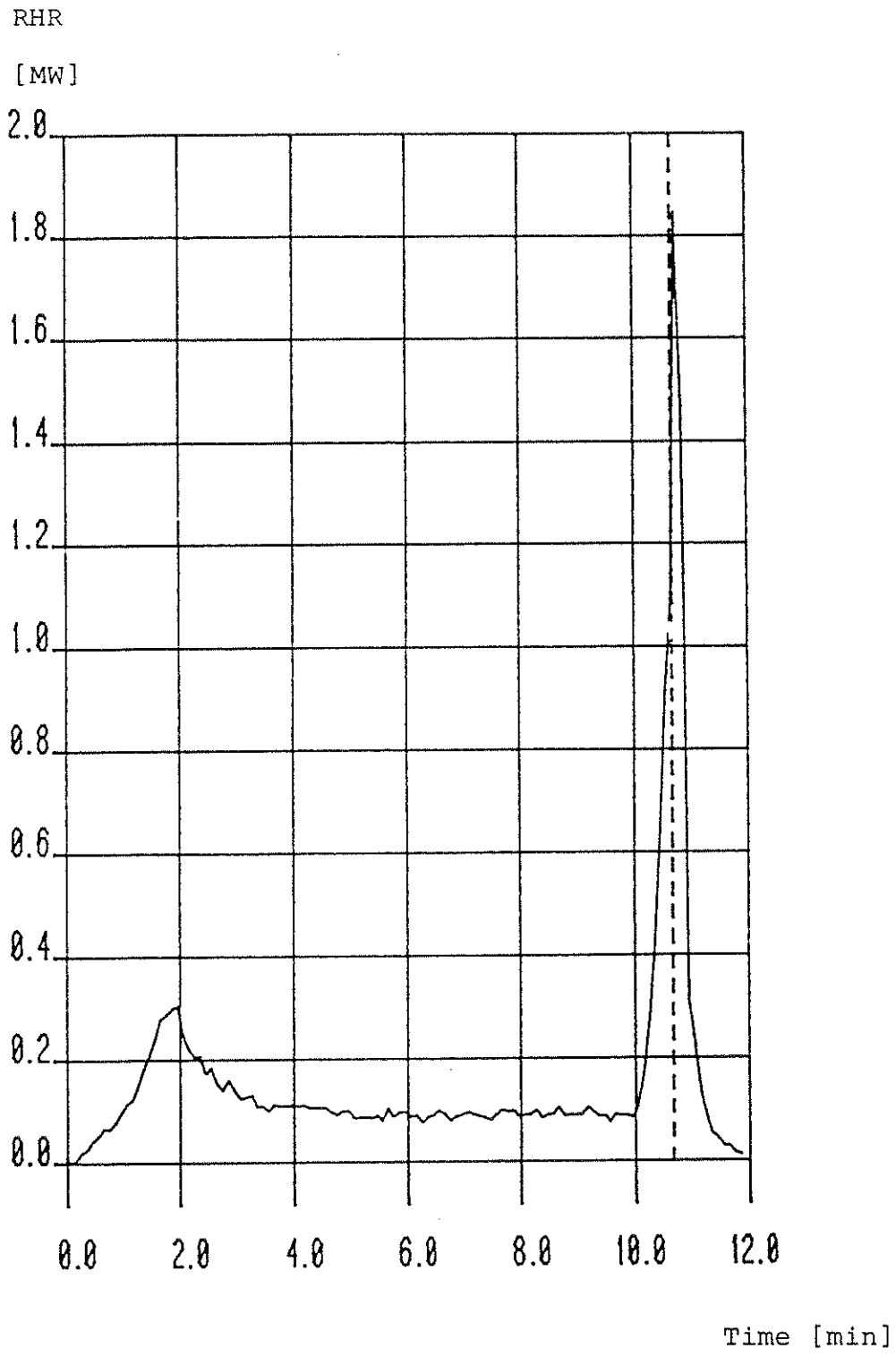

FIG. 10 Experimental heat output curve for full scale room test with material 7

Material 8

Textile wallcovering on mineral wool

------- flashover

RHR

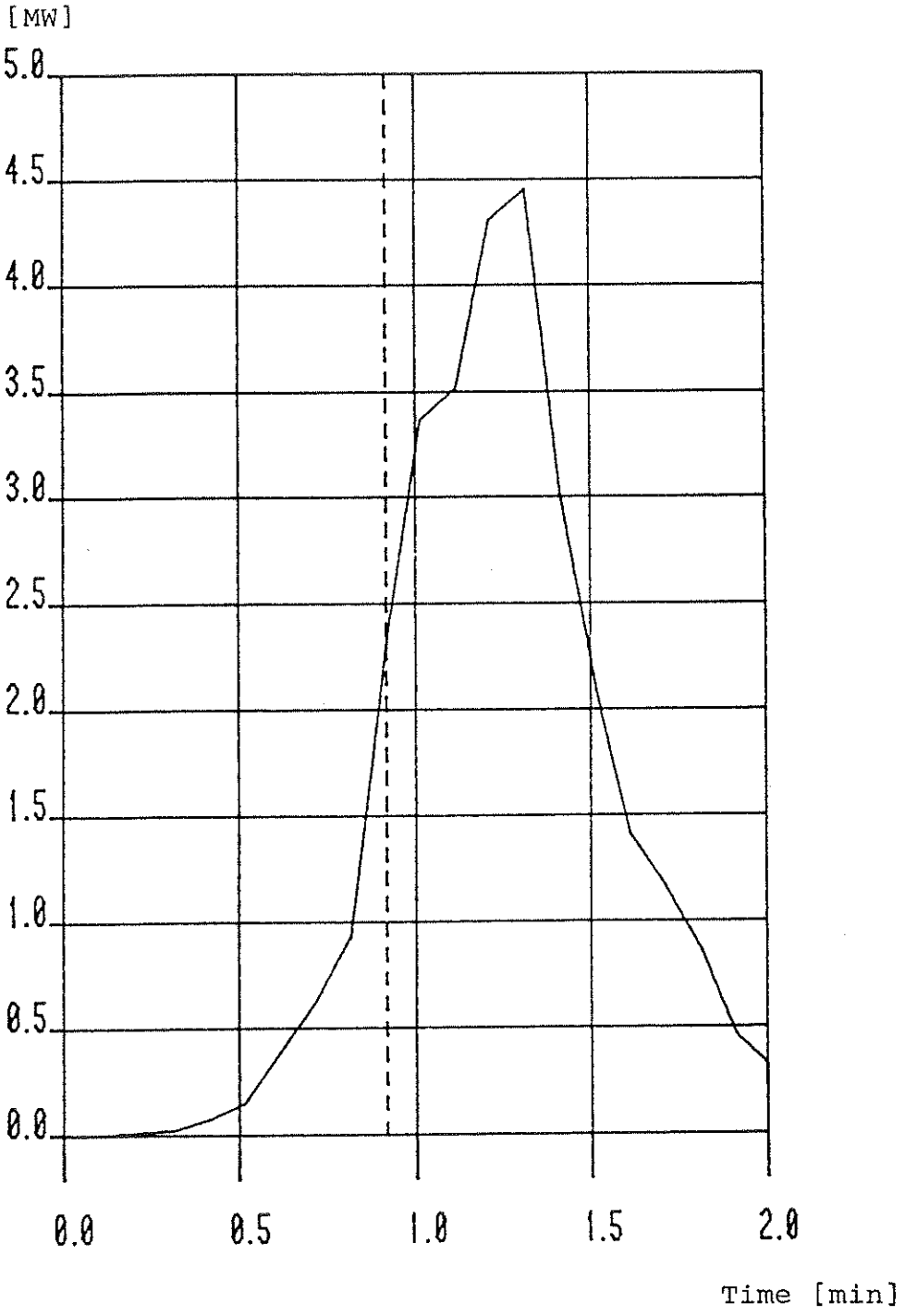

FIG. 10 Experimental heat output curve for full scale room test with material 8

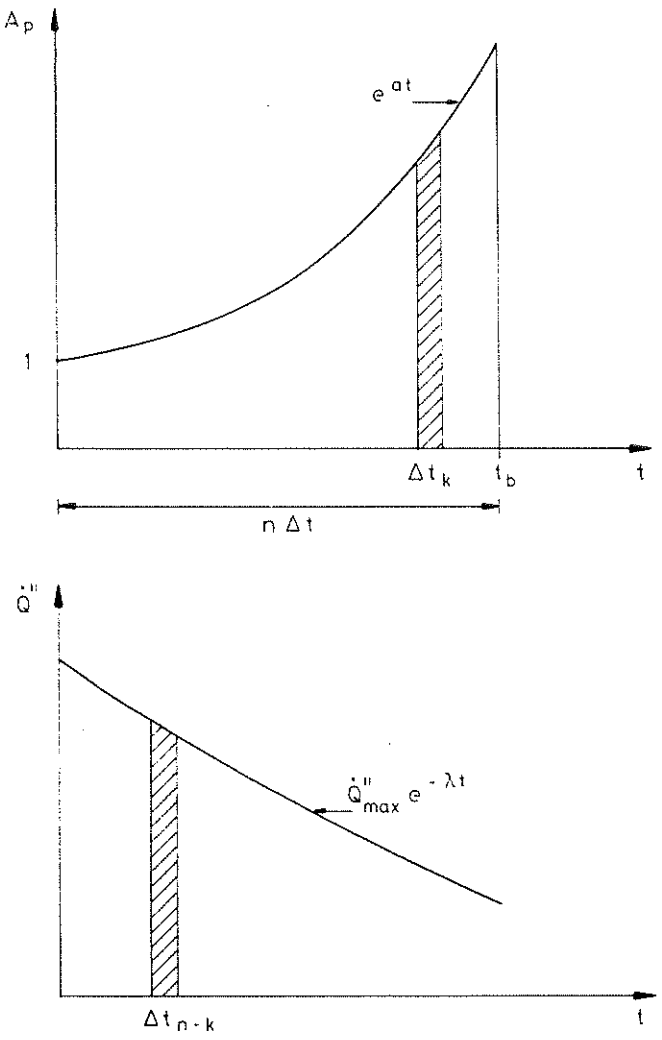

FIG. 11 Principle behind superposition integral in Eq. 21

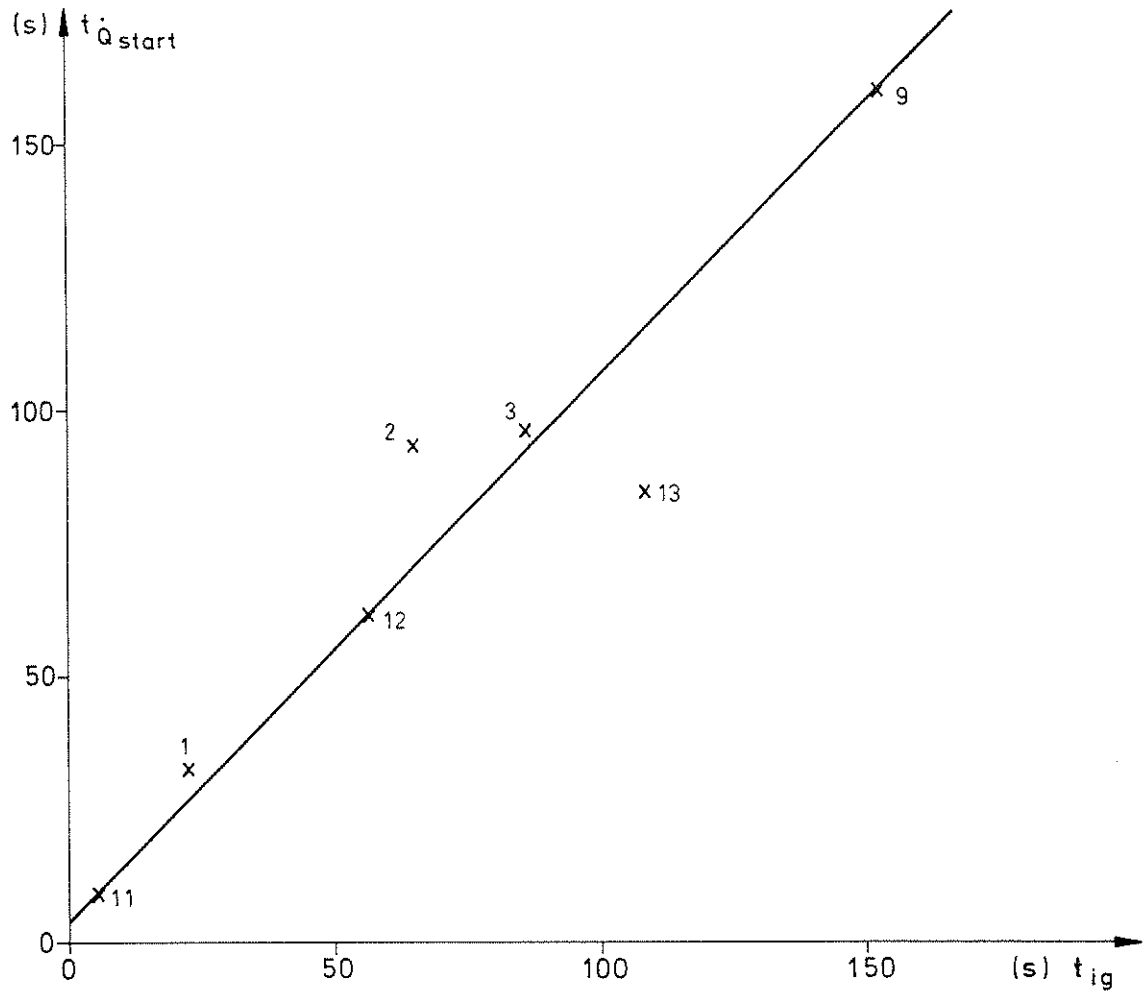

FIG. 12 Relation between response time of room test RHR-measurement system and specimen ignitability time at 30 kW/m^2

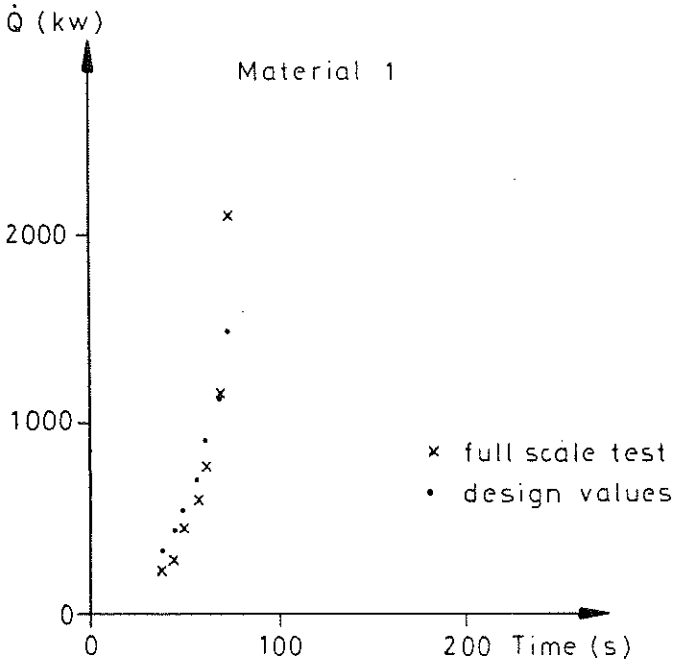

a)

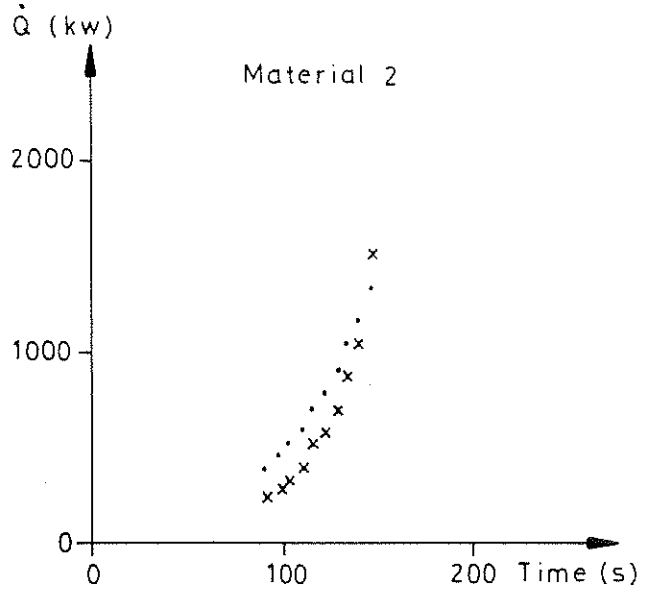

b)

FIG. 13a-g Experimental RHR curves from room test (x) and design theory curves (·). The curve with ° in Fig. g denotes calculated values where response time = experimental value

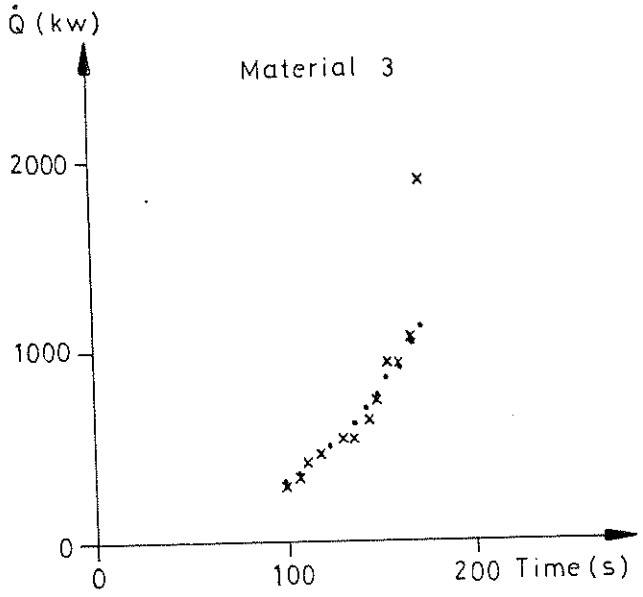
Q̇ (kw)
Material 3
2000
1000
0
0
100
200 Time (s)

c)

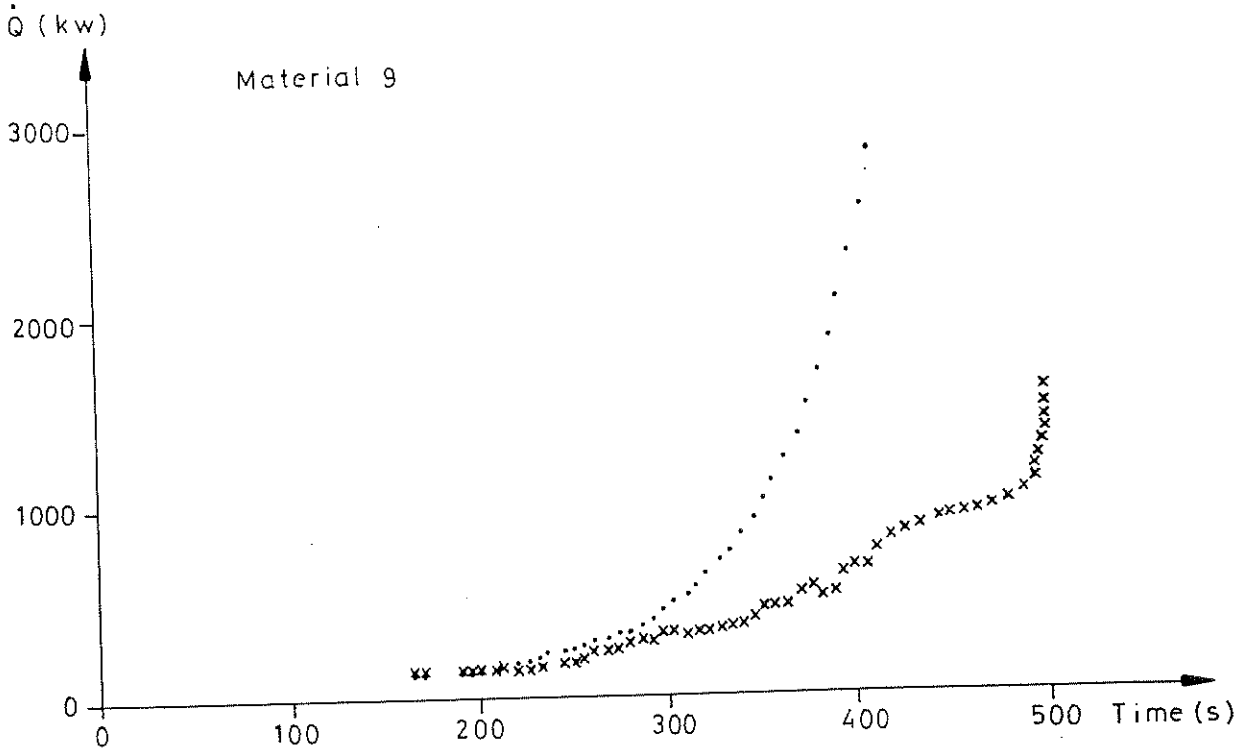
Q̇ (kw)
Material 9
3000
2000
1000
0
0
100
200
300
400
500 Time (s)

d)

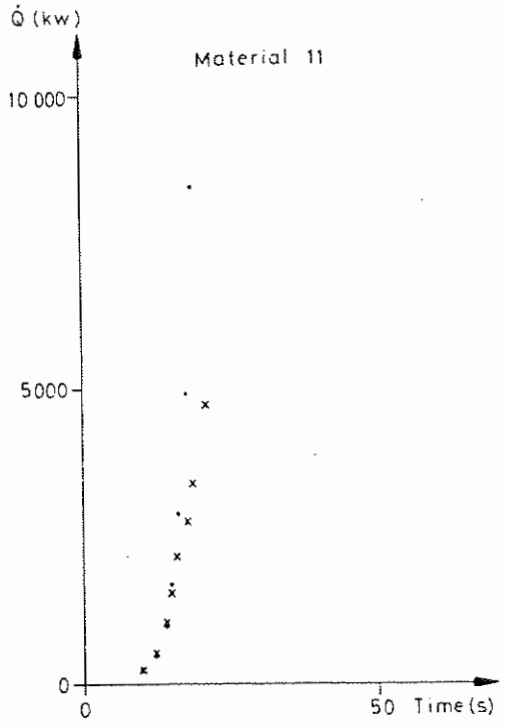
Q̇ (kw)
Material 11
10 000
5000
0
0
50 Time(s)

e)

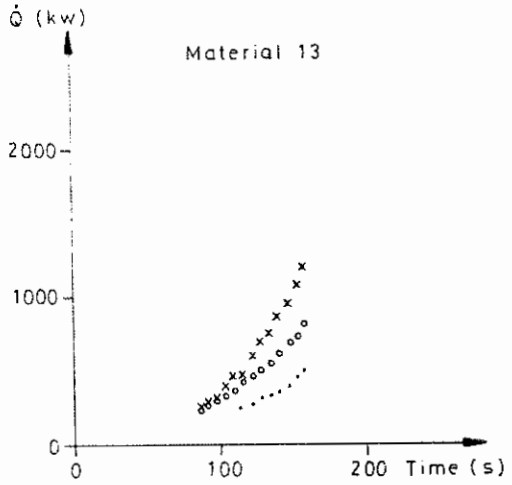
Q̇ (kw)
Material 13
2000
1000
0
0
100
200 Time (s)

g)

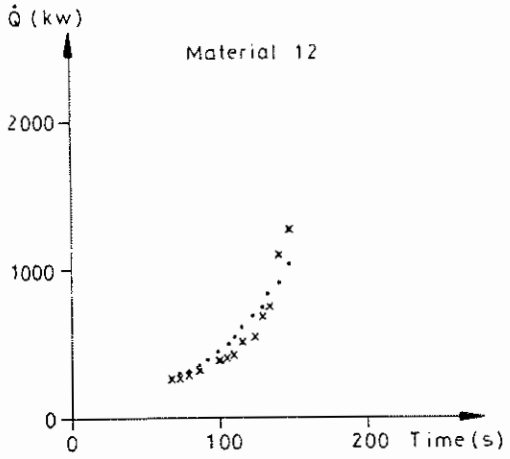
Q̇ (kw)
Material 12
2000
1000
0
0
100
200 Time(s)

f)

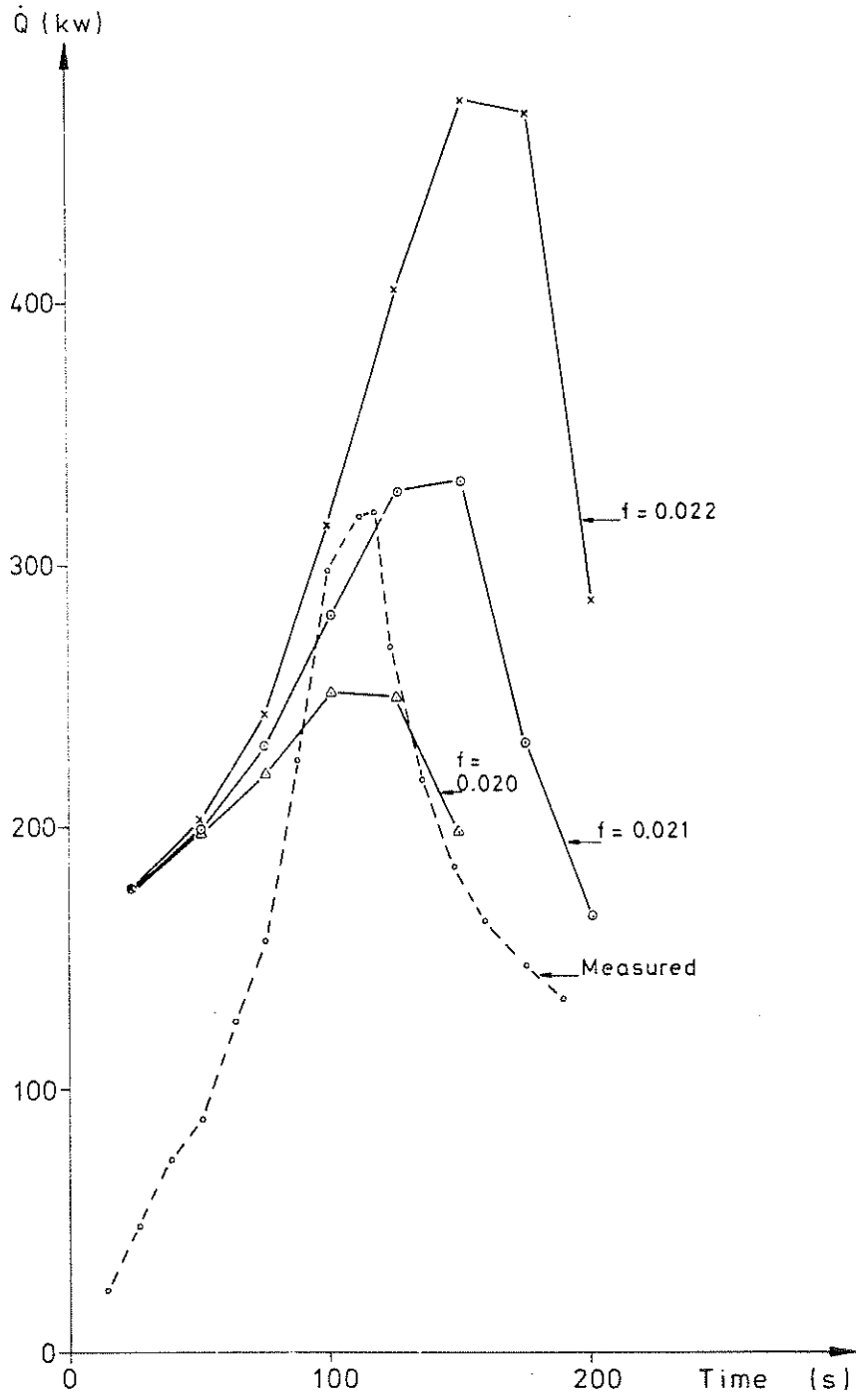

FIG. 14 Experimental and calculated RHR curves for room test material 7